DIFFERENTIAL SPATIAL MODULATION: LOW COMPLEXITY DETECTION AND IMPROVED ERROR PERFORMANCE

Kavish Kadathlal

Supervisor: Prof. Hongjun Xu

Co-Supervisor: Dr. Narushan Pillay

Submitted in fulfilment of the degree of Master of Science in Engineering,

College of Agriculture, Engineering and Science, School of Engineering, University of KwaZulu-Natal, Durban, South Africa

December 2016

As the candidate's supervisor, I agree to the submission of this dissertation.

Date of Submission: _____

Supervisor: _____

Prof. Hongjun Xu

Declaration 1 - Plagiarism

I, **Kavish Kadathlal,** declare that:

1. The research reported in this thesis, except where otherwise indicated, is my original research.
2. This thesis has not been submitted for any degree or examination at any other university.
3. This thesis does not contain other persons' data, pictures, graphs or other information, unless specifically acknowledged as being sourced from other persons.
4. This thesis does not contain other persons' writing, unless specifically acknowledged as being sourced from other researchers. Where other written sources have been quoted, then:
    a. Their words have been re-written but the general information attributed to them has been referenced
    b. Where their exact words have been used, then their writing has been placed in italics and inside quotation marks, and referenced.
5. This thesis does not contain text, graphics or tables copied and pasted from the Internet, unless specifically acknowledged, and the source being detailed in the thesis and in the References sections.

Signed: _____

Kavish Kadathlal

Declaration 2 - Publications

DETAILS OF CONTRIBUTION TO PUBLICATIONS that form part and/or include research presented in this thesis (include publications in preparation, submitted, *in press* and published and give details of the contributions of each author to the experimental work and writing of each publication)

Publication 1:

K. Kadathlal, H. Xu, and N. Pillay, "A Generalized Differential Scheme for Spatial Modulation Systems," *IET Commun.*, [prepared for second review], Dec. 2016.

Publication 2:

H. Xu, K. Kadathlal, and N. Pillay, "A Simple Low-Complexity Near-ML Detection Scheme for Differential Spatial Modulation," *SAIEE Africa Research Journal*, [under review], Dec. 2016.

Signed: _____

Kavish Kadathlal

Acknowledgements

I would like to convey my sincere gratitude to my supervisor, Professor Hongjun Xu, for his continued guidance, motivation and support throughout the completion of this work. His in-depth knowledge of the subject matter, and passion for research has been inspiring.

I would also like to thank my co-supervisor, Dr Narushan Pillay, for inspiring me in my undergraduate years to pursue an MSc. degree, and for his resolute academic guidance and assistance throughout the completion of this work.

My thanks go to my family for their unwavering support during the difficult times, and for presenting me with the opportunity to complete my postgraduate studies.

Finally, the financial assistance of the National Research Foundation (NRF) towards this research is hereby acknowledged. Opinions expressed and conclusions arrived at, are those of the author and are not necessarily to be attributed to the NRF.

Abstract

Multiple-input multiple-output (MIMO) systems utilize multiple transmit and receive antennas in order to achieve a high spectral efficiency and improved reliability for wireless links. However, MIMO systems suffer from high system complexity and costs, due to inter-channel interference (ICI) at the receiver, the requirement of transmit-antenna synchronization (TAS), and the need for multiple radio frequency (RF) chains.

Spatial modulation (SM) is a MIMO system which maintains a high spectral efficiency without suffering from ICI or TAS, while utilizing a single RF chain. However, the SM receiver requires full knowledge of the channel state information (CSI) to achieve optimal error performance, thereby increasing the receiver detection complexity.

To overcome this, differential SM (DSM) has been developed which does not require CSI to perform detection. However, the maximum-likelihood (ML) detection for DSM results in excessive computational complexity when the number of transmit antennas is large, and suffers from a 3 dB signal-to-noise ratio (SNR) penalty compared to coherent SM.

This dissertation aims to reduce the computational complexity of DSM, and mitigate the 3 dB SNR penalty. A generalized differential scheme based on SM (GD-SM) is proposed, which employs optimal power allocation to reduce the 3 dB SNR penalty. GD-SM divides a frame into a reference part and normal part. The reference part is transmitted at a higher power than the normal part, and is used to encode and decode the information in the normal part. Optimal power allocation is applied to the system, and the results demonstrate that at a bit error rate (BER) of 10^{-5} and for a frame length of 400, GD-SM is only 0.5 dB behind coherent SM.

The frame structure of GD-SM and optimal power allocation is extended to conventional DSM (C-DSM). At a BER of 10^{-5}, a 2.5 dB gain is achieved over C-DSM for a frame length of 400. Furthermore, the frame structure allows for easy implementation of quadrature amplitude modulation (QAM), which yields an additional gain in error performance. The use of QAM constellations is not possible in C-DSM.

A simple, near-ML, low-complexity detector (L-CD) is proposed for DSM. The L-CD exploits the features of the phase shift keying, and amplitude phase shift keying constellations to achieve near-ML error performance, and at least a 98% reduction in computational complexity. The proposed detector is independent of the constellation size, and demonstrates a significantly lower complexity than that of current L-CDs.

Table of Contents

List of Figures

List of Tables

Glossary of Acronyms

ABEP	Average Bit Error Probability
AF	Amplify-and-Forward
AI	Antenna Index
AM	Antenna Matrix
APM	Amplitude and/or Phase Modulation
AWGN	Additive White Gaussian Noise
BER	Bit Error Rate
CSI	Channel State Information
D-BLAST	Diagonal-Bell Laboratories Layered Space-Time
DSM	Differential Spatial Modulation
GDM	Generalized Differential Modulation
GD-SM	Generalized Differential scheme for Spatial Modulation
G-DSM	Generalized Differential Spatial Modulation
HL-ML	Hard-Limiter Maximum Likelihood
IAS	Inter-Antenna Synchronization
ICI	Inter-Channel Interference
i.i.d	Independent and Identically Distributed
M-M APSK	M-ary - M-ary Amplitude Phase Shift Keying
MIMO	Multiple-Input Multiple Output
ML	Maximum Likelihood
M-PSK	M-ary Phase Shift Keying
M-QAM	M-ary Quadrature Amplitude Modulation
MSDD	Multiple-Symbol Differential Detection
PEP	Pairwise Error Probability
RF	Radio Frequency
SISO	Single-Input Single-Output
SM	Spatial Modulation
SNR	Signal-to-Noise Ratio
STBC	Space-Time Block Code
QoS	Quality of Service
V-BLAST	Vertical-Bell Laboratories Layered Space-Time

Part I

Introduction

1. Introduction

Wireless communications is the preferred method with which we communicate [1], and continues to experience rapid growth, making it the fastest growing segment in the communications industry [2-3]. This is due to the exponential growth in mobile cellular systems, which has led to an increase in voice traffic [2], as well as an increase in the use of data services, such as broadband internet, multimedia streaming, video teleconferencing, and file transfer [2].

Thus, there is an increased demand for higher data rates and improved quality of service (QoS), which has directly led to the need for wireless systems with improved spectral efficiency and reliability [3]. However, in order to meet these requirements, designers need to overcome various challenges, namely, limited spectrum availability and complex fading environments [3].

The use of multiple receive antennas is one method employed to reduce the effects of noise and fading, thereby improving the reliability of the wireless system without affecting the bandwidth of the transmitted signal [4]. Moreover, the use of multiple transmit antennas allows the wireless system to achieve higher data rates through the transmission of multiple data streams [4]. Consequently, there is considerable research carried out on multiple-input multiple-output (MIMO) wireless communication systems.

In the subsequent subsections, a brief description is provided of the technology used in some form within this dissertation.

1.1. Multiple-Input Multiple-Output Systems

MIMO systems are regarded as one of the most significant breakthroughs in the communications industry, as it provides a solution to the bottleneck of traffic capacity experienced in wireless communication systems [5]. MIMO, unlike single-input single-output (SISO) systems, makes use of multiple transmit and receive antennas, which permits transmission and reception of multiple data streams concurrently. Improved error performance and throughput may be achieved over a SISO system via spatial multiplexing, spatial diversity, or a combination of both [6-7].

The diagonal-Bell Laboratories layered space-time (D-BLAST) and vertical-BLAST (V-BLAST) architectures in [8-9], respectively, exploit spatial multiplexing in MIMO systems to realize spectral efficiencies of up to 20-40 bits/s/Hz. However, the use of spatial multiplexing requires that the transmit antennas be synchronized during transmission [6-7], since the detector assumes that transmission from the antennas occurs simultaneously [6]. Furthermore, spatial multiplexing results in inter-channel interference (ICI) at the receiver, which degrades the error performance of the wireless link. However, ICI may be reduced by providing sufficient spacing among the transmit and receive antennas [10].

Spatial diversity is utilized to improve the reliability of wireless links [6]. However, schemes incorporating spatial diversity still require inter-antenna synchronization (IAS), and may suffer from ICI at the receiver. In [11], an Alamouti scheme based on a MIMO system with two transmit antennas is presented, which achieves spatial diversity at the transmitter. The proposed system improves the reliability of the wireless link, albeit at a lower data rate, since transmission and demodulation of two symbols occurs over a period of two time slots.

MIMO systems also require multiple radio frequency (RF) chains, usually one for each transmit antenna. This, coupled with ICI and IAS, leads to increased complexity and costs, as well as lower energy efficiency. However, since the advantages of MIMO are substantial, research is conducted into MIMO systems which have reduced complexity and costs, while maintaining the advantages of MIMO.

1.2. Spatial Modulation

Spatial modulation (SM) [12-15] is a newly developed, spectrally efficient, transmission technique based on MIMO. SM, unlike conventional MIMO systems, only activates a single transmit antenna in a given time slot, in order to convey information. The remaining transmit antennas, transmit zero power [12-13]. The advantage of this, is that SM requires no IAS at the transmitter, and is capable of completely avoiding ICI at the receiver. Furthermore, since SM only activates a single antenna in each time instant, only a single RF chain is required for the system [14]. As a result, SM incurs reduced costs and overall complexity relative to existing MIMO systems, and is capable of outperforming MIMO systems such as V-BLAST [12, 15].

SM maintains a relatively high spectral efficiency compared to conventional MIMO schemes. For an SM system with N_t transmit antennas and N_r receive antennas, as shown in Figure 1, the high spectral efficiency is achieved by mapping the information bits to an amplitude and/or phase modulated (APM) symbol in the signal domain, and a specific transmit antenna index, which determines the activated transmit antenna in the spatial domain. It is noted that the information mapped to the spatial domain is not transmitted explicitly, but rather via the index of the activated transmit antenna [7]. Furthermore, the APM symbol may be drawn from an M-ary quadrature amplitude modulation (M-QAM) or M-ary phase shift keying (M-PSK) constellation.

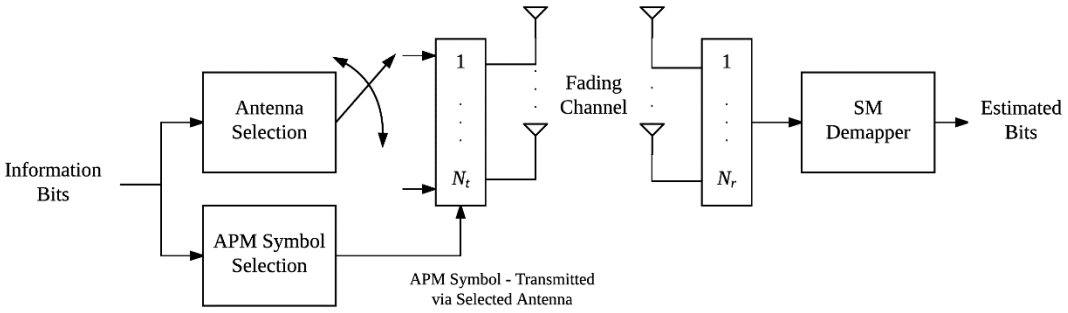

Figure 1: System Model of SM [14].

Similarly to conventional MIMO schemes, SM performs coherent detection, which therefore, requires that the receiver has full knowledge of the channel state information (CSI). In [16], it is concluded that the error performance of SM is more robust than V-BLAST when in the presence of channel estimation errors. However, channel estimation errors in SM are still inevitable, thus error performance penalties are expected [16-17]. This is evident in high mobility conditions, wherein the fading environment rapidly changes [17-18]. Obtaining the precise CSI in such conditions results in performance limitations imposed by high processing complexity, and considerable pilot overhead and channel estimation errors [17-18].

1.3. Differential Spatial Modulation

Differential spatial modulation (DSM) [18-21] is a MIMO system which utilizes a similar architecture to that of SM, wherein at any time instant, only a single transmit antenna is activated to convey information. As a result, DSM is able to maintain the merits of SM over conventional MIMO systems.

In DSM, APM symbols are first differentially encoded, then transmitted via a space-time block. The information bits are mapped to N_t APM symbols, and one antenna matrix (AM), out of a total of Q AMs. The AM is utilized to govern the order in which the N_t transmit antennas are activated over N_t time slots. Thereafter, based on the selected AM, the N_t transmit antennas convey N_t APM symbols within the N_t time slots. The APM symbols are differentially encoded based on the symbols transmitted in the previous space-time block, and are drawn from an M-PSK or M-M amplitude phase shift keying (APSK) constellation, the latter of which allows for improved spectral efficiency [21]. The DSM schemes in [18-21] do not permit the use of QAM modulation, as it is not compatible with the differential process.

By nature, the DSM detection process is non-coherent, thus, knowledge of the CSI is not required for the maximum likelihood (ML) detector to achieve optimal error performance. This reduces the processing complexity of DSM, and furthermore, there are no performance penalties incurred as a result of pilot overheads and channel estimation errors. However, due to the non-coherent detection process, DSM does suffer from a 3 dB error performance penalty compared to coherent SM. Additionally, the computational complexity, which is the number of real-valued multiplications in an algorithm [22], of the DSM ML detector grows exponentially with an increase in N_t.

This excessive computational complexity has prompted research into low-complexity detection schemes for DSM. In [22-23], low-complexity detectors have been proposed for DSM with M-PSK modulation, which achieve significant computational complexity reductions over the ML detector. However, the detector in [22] sacrifices error performance for lower computational complexity or vice versa, when N_t is large; while the detector in [23] offers suboptimal error performance, and whose computational complexity is dependent upon the size of the M-PSK constellation. Furthermore, the algorithms in [22-23] are complicated to execute.

In [24], a multiple-symbol differential detection (MSDD) scheme is proposed for spatial modulation. The MSDD scheme observes multiple received space-time blocks, to determine the information contained in a single space-time block. The scheme achieves a considerable gain in error performance over conventional DSM, however, this comes at the cost of exorbitant computational complexity.

1.4. Generalized Differential Modulation

Generalized differential modulation (GDM) has been introduced in [25-26] for differential schemes using space-time block codes (STBC) and amplify-and-forward (AF) relay networks, respectively. The proposed GDM schemes are capable of reducing the error performance penalty incurred through non-coherent detection.

In both schemes, the transmitted frame begins with reference block which conveys no information, and is succeeded by normal, information conveying blocks, which fill the remainder of the frame. The reference block and normal blocks are differentially encoded based on the previous and current reference block, respectively. Additionally, the receiver utilizes the reference signal to retrieve the information contained within the following normal blocks.

Based on this frame structure, the schemes allocate more of the transmit power to the reference block as compared to the subsequent normal blocks. As a result, the received reference signal provides the receiver with an improved estimation of the combined channel matrix [25-26].

Therefore, the estimation-detection carried out via the ML detector achieves improved error performance, as compared to conventional differential modulation with equal power allocated among all blocks [25-26].

2. Motivation and Research Objective

DSM [18-21] is an attractive MIMO-based alternative to coherent SM, as its detector does not require the CSI to perform detection. Additionally, DSM achieves a relatively high spectral efficiency compared to SM, and does not suffer from the performance limiting factors such as IAS and ICI [19-20]. Therefore, DSM is a promising transmission scheme which may be employed in future mobile and fixed wireless communication systems.

The ML detector utilized in DSM, however, does experience exponential growth in computational complexity when the number of transmit antennas increase [23]. This is due to the fact that the ML detector performs an exhaustive search through all possible combinations of the Q AMs and N_t APM symbols.

Furthermore, the non-coherent detection results in a 3 dB error performance penalty compared to coherent SM [18]. Also, unlike coherent SM, DSM is unable to make use of the power and spectrally efficient QAM constellation.

Low-complexity detectors have been proposed for DSM in [22] and [23], each of which has its own advantages and disadvantages. The existing low-complexity detectors either sacrifice error performance for lower computational complexity or vice versa, or are suboptimal in their error performance and still realize high computational complexity due to dependence upon the system configuration. Furthermore, the algorithms are complicated to execute.

Additionally, the MSDD scheme developed for DSM to alleviate the 3 dB error performance in [24], suffers from exorbitant computational complexity.

Motivated by the above, this dissertation aims to provide a low-complexity detector, whose error performance is the same as that of the ML detector; and whose computational complexity is considerably lower than the ML and current low-complexity detectors in [22-23], while being independent of the system configuration.

The second objective is to develop an easily implementable DSM system, capable of mitigating the 3 dB error performance gap relative to SM, without incurring additional computational complexity. Additionally, the theoretical error performance of the DSM system must be derived to validate the improvement achieved in error performance.

The outcomes of the research conducted are presented in Papers A and B, which follow.

3. Contributions of Included Papers

3.1. Paper A

K. Kadathlal, H. Xu, and N. Pillay, "A Generalized Differential Scheme for Spatial Modulation Systems," *IET Commun.*, [prepared for second review], Dec. 2016.

In Paper A, the system models of SM and DSM are first presented. Thereafter, a generalized differential scheme for SM (GD-SM) is introduced, together with the optimal ML detector. The frame structure and optimal power allocation employed in GD-SM is then given in detail. Furthermore, the frame structure and power allocation concept used in GD-SM is extended to conventional DSM, thus a generalized DSM (G-DSM) scheme is formulated. An upper bound on the average bit error probability is provided for both proposed schemes. The complexity of the ML detectors for the various schemes, are analyzed and discussed. Finally, simulation and theoretical results are presented for GD-SM and G-DSM, with M-PSK and M-QAM modulation, and varying constellation sizes and antenna configurations. The results demonstrate a considerable improvement in error performance over the respective differential system without optimal power allocation. Additionally, the derived theoretical upper bound on the average bit error probability closely matches the simulation results at high signal-to-noise ratios (SNRs).

3.2. Paper B

H. Xu, K. Kadathlal, and N. Pillay, "A Simple Low-Complexity Near-ML Detection Scheme for Differential Spatial Modulation," *SAIEE Africa Research Journal*, [under review], Dec. 2016.

Paper B aims to reduce the computational complexity incurred by the DSM ML detector, for PSK and APSK modulation. Firstly, the DSM systems for PSK and APSK modulation are presented together with expressions for the respective optimal ML detector. Thereafter, the current low-complexity detectors, identified in the literature, are discussed. A simple low-complexity detector is then presented for DSM with M-PSK modulation, and the proposed algorithm is modified and applied to DSM with M-M APSK modulation. A complexity analysis demonstrates that the proposed detectors achieve a considerable reduction in computational complexity over their respective ML detector and existing low-complexity detectors. Finally, simulation results are presented for M-PSK and M-M APSK modulation, with various transmit and receive antenna configurations. It is shown that the proposed detector achieves optimal ML error performance throughout the SNR range, with a significantly reduced computational complexity.

4. Future Work

The upper bound on the ABEP derived in Paper A for GD-SM and G-DSM does not closely match the simulated error performance results at low SNRs. Therefore, there is a need for a simple, closed form theoretical solution, which provides an exact match to the simulated error performance of the proposed systems, throughout the SNR range. Additionally, this solution should provide an exact match irrespective of the system configuration.

References

[1] M. K. Simon, and M. S. Alouini, *Digital Communication over Fading Channels: A Unified Approach to Performance Analysis*, New York: John Wiley & Sons, Inc., 2000.

[2] A. Goldsmith, *Wireless Communications*, Cambridge University Press, 2005.

[3] A. Paulraj, R. Nabar, and D. Gore, *Introduction to Space-Time Wireless Communications*, Cambridge University Press, 2003.

[4] J. G. Proakis, and M. Salehi, *Digital Communications*, (5th ed.), New York: McGraw-Hill, 2008.

[5] D. Gesbert, M. Shafi, D. Shiu, P. J. Smith, and A. Naguib, "From Theory to Practice: An Overview of MIMO Space-Time Coded Wireless Systems," *IEEE J. Sel. Areas Commun.,* vol. 21, no. 3, pp. 281 – 302, Apr. 2003.

[6] J. Jeganathan, A. Ghrayeb, L. Szczencinski, and A. Ceron, "Space Shift Keying Modulation for MIMO," *IEEE Trans. Wireless Commun.*, vol. 8, no. 7, pp. 3692 – 3703, Jul. 2009

[7] N. Pillay, and H. Xu, "Low-Complexity Detection and Transmit Antenna Selection for Spatial Modulation," *SAIEE Africa Research J.,* vol. 105, no. 1, pp. 4 – 12, Mar. 2014.

[8] G. J. Foschini, "Layered Space-Time Architecture for Wireless Communication in a Fading Environment When Using Multi-Element Antennas," *Bell Labs Tech. J.,* vol. 1, no. 2, pp. 41 – 59, 1996.

[9] P. W. Wolniansky, G. J. Foschini, G. D. Golden, and R. A. Valenzuela, "V-BLAST: An Architecture for Realizing Very High Data Rates Over the Rich-Scattering Wireless Channel," *in 1998 URSI ISSE*, pp. 295 – 300, Oct. 1998.

[10] S. Loyka, and G. Tsoulos, "Estimating MIMO System Performance Using the Correlation Matrix Approach," *IEEE Commun. Lett.,* vol. 6, no. 1, pp. 19 – 21, Jan. 2002.

[11] S. M. Alamouti, "A Simple Transmit Diversity Technique for Wireless Communications," *IEEE J. Sel. Areas Commun*, vol. 16, no. 8, pp. 1451 – 1458, Oct. 1998.

[12] R. Y. Mesleh, H. Haas, C. W. Ahn, and S. Yun, "Spatial Modulation – A New Low Complexity Spectral Efficiency Enhancing Technique," *in Proc. of the Conf. on Commun. and Netw., China*, pp. 1 – 5, Oct. 2006.

[13] R. Y. Mesleh, H. Haas, S. Sinanovic, C. W. Ahn, and S. Yun, "Spatial Modulation," *IEEE Trans. Veh. Tech.*, vol. 57, no. 4, pp. 2228 – 2241, Jul. 2008.

[14] R. Rajashekar, K. V. S. Hari, and L. Hanzo, "Spatial Modulation Aided Zero-Padded Single Carrier Transmission for Dispersive Channels," *IEEE Trans. Commun.*, vol. 61, no. 6, pp. 2318 – 2329, Jun. 2013.

[15] J. Jeganathan, A. Ghrayeb, and L. Szczencinski, "Spatial Modulation: Optimal Detection and Performance Analysis," *IEEE Commun. Lett.*, vol. 12, no. 8, pp. 545 – 547, Aug. 2008.

[16] E. Basar, U. Aygolu, E. Panayirci, and H. V. Poor, "Performance of Spatial Modulation in the Presence of Channel Estimation Errors," *IEEE Commun. Lett.*, vol. 16, no. 2, pp. 176 – 179, Feb. 2012.

[17] S. Sugiura, S. Chen, and L. Hanzo, "Coherent and Differential Space-Time Shift Keying: A Dispersion Matrix Approach," *IEEE Trans. Commun*., vol. 58, no. 11, pp. 3219 – 3230, Nov. 2010.

[18] Y. Bian, X. Cheng, M. Wen, L. Yang, H. V. Poor, and B. Jiao, "Differential Spatial Modulation," *IEEE Trans. Veh. Technol.*, vol. 64, no. 7, pp. 3262 – 3268, Jul. 2015.

[19] Y. Bian, M. Wen, X. Cheng, H. V. Poor, and B. Jiao, "A Differential Scheme for Spatial Modulation," *in Proc. 2013 IEEE GLOBECOM*, pp. 3925 – 3930, Dec. 2013.

[20] N. Ishikawa, and S. Sugiura, "Unified Differential Spatial Modulation," *IEEE Wireless Commun. Lett.*, vol. 3, no. 4, pp. 337 – 340, Aug. 2014.

[21] P.A. Martin, "Differential Spatial Modulation for APSK in Time-Varying Fading Channels," *IEEE Commun. Lett*., vol. 19, no. 7, pp. 1261 – 1264, Apr. 2015.

[22] L. Xiao, P. Yang, X. Lei, Y. Xiao, S. Fan, S. Li, and W. Xiang, "A Low-complexity Detection Scheme for Differential Spatial Modulation," *IEEE Commun. Lett*., vol. 19, no. 9, pp. 1516 – 1519, Jun. 2015.

[23] M. Wen, X. Cheng, Y. Bian, and H. V. Poor, "A Low-Complexity Near-ML Differential Spatial Modulation Detector," *IEEE Signal Process. Lett*., vol. 22, no. 11, pp. 1834 – 1838, Jun. 2015.

[24] T. P. Nguyen, M. T. Le, and X. N. Tran, "Multiple-Symbol Differential Detection for Spatial Modulation," *REV J. Electron. and Commun.*, vol. 5, no. 1 – 2, pp. 22 – 28, Jan. 2015.

[25] L. Li, Z. Fang, Y. Zhu, and Z. Wang, "Generalized Differential Transmission for STBC Systems," *in Proc. 2008 IEEE GLOBECOM*, pp. 1 – 5, Dec. 2008.

[26] Z. Fang, L. Li, X. Bao, and Z. Wang, "Generalized Differential Modulation for Amplify-and-Forward Wireless Relay Networks," *IEEE Trans. Veh. Tech.*, vol. 58, no. 6, pp. 3058 – 3062, Jul. 2009.

Part II

Included Papers

Paper A: A Generalized Differential Scheme for Spatial Modulation Systems

K. Kadathlal, H. Xu, and N. Pillay

Prepared for second review, IET Communications.

Abstract

Spatial modulation (SM) is an efficient transmission scheme based on multiple-input multiple-output systems. SM, by nature, requires coherent detection to achieve optimal error performance. This requires that the receiver has full knowledge of the channel state information (CSI), however, determining the CSI results in an increase in the detection complexity at the receiver. Differential modulation systems are capable of performing detection without knowledge of the CSI at the receiver, however, they suffer a 3 dB error performance penalty as compared to their coherent counterparts. In this paper, we present a generalized differential scheme for spatial modulation (GD-SM) based on generalized differential modulation, which is capable of reducing the performance penalty incurred through optimal power allocation. Furthermore, we extend the architecture of GD-SM and optimal power allocation to conventional differential spatial modulation. The architecture of the proposed systems, advantageously permits the use of either M-ary quadrature amplitude modulation or M-ary phase shift keying constellations. Simulation and theoretical results demonstrate that GD-SM incurs only about 0.5 dB performance loss as compared to coherent SM when the frame length is 400.

1. Introduction

Spatial Modulation (SM) is a high-rate, spectrally efficient multiple-input multiple-output (MIMO) transmission scheme, which utilizes the transmit antenna index in addition to a standard modulated symbol to convey information [1]. SM when compared to conventional MIMO systems requires no transmit antenna synchronization and is capable of eliminating inter-channel interference (ICI) at the receiver, since only one transmit antenna is active at any time instant [1-2]. However, for optimal error performance, the receiver in an SM system requires full knowledge of the channel state information (CSI) to perform coherent detection. This increases detection complexity at the receiver as well as limitations imposed by pilot overhead and channel estimation errors [3].

Differential spatial modulation (DSM) [3-5] is an attractive alternative to coherent spatial modulation, since it does not require CSI to perform detection, while maintaining the advantages of SM over conventional MIMO systems. However, due to the differential encoding process at the transmitter and non-coherent detection at the receiver, DSM suffers an approximate 3 dB error performance penalty as compared to an SM system of equal spectral efficiency [4-5].

In [6-7], generalized differential modulation (GDM) schemes are proposed, which are capable of reducing the error performance penalty incurred through non-coherent detection. Liangbin *et al.* [6] provide a GDM scheme for space-time block code (STBC) systems, wherein the transmitted frames are divided into a reference block and normal blocks, both of which are differentially encoded based on the previous and current reference block, respectively. It is noted that the reference and normal blocks are both used to convey information from the source to destination. The improvement in error performance is achieved by allocating more transmit power to the reference block as compared to the normal blocks, resulting in an improved estimation of the combined channel matrix during demodulation [6]. In [7], Fang *et al.* apply a similar GDM frame architecture to [6] in order to bridge the gap between coherent and non-coherent modulation for amplify-and-forward (AF) relay networks.

The concept of power allocation between the reference and normal blocks is studied in [6-7], in order to maximize the average output signal-to-noise ratio (SNR) of the respective systems. On this note, an optimization problem is formulated in both [6] and [7], to which optimal solutions are derived using Lagrange multipliers. The optimal power allocation presented in [7] is similar to that of [6], however unlike [6], it is dependent upon the statistics of the differential modulation scheme. In [6-7], it is observed that the error performance may also be improved by increasing the frame length, since the power allocated to the reference block is increased. This holds true, provided that the channel remains unchanged for the duration of the frame.

Motivated by the GDM works in [6-7], we propose a generalized differential scheme for SM (GD-SM) based on the concept of power allocation. Each frame in the proposed scheme consists of a reference block and normal blocks, of which only the normal blocks convey information. The normal blocks are differentially encoded based on the reference block, however, unlike in [6-7], the reference block is not differentially-encoded based on the previous reference block, and rather it remains constant throughout transmission. This property provides an option for the information carrying symbols in the normal-block to be drawn from either an M-ary phase shift keying (M-PSK) or M-ary quadrature amplitude modulation (M-QAM) constellation, the latter of which requires no complicated encoding algorithms to achieve a suitable constellation for use in differential modulation. This is advantageous as M-QAM is more spectrally and power efficient than M-PSK [8].

Furthermore, we extend the structure and power allocation concept used in GD-SM to conventional DSM, and thus, we present a generalized scheme for differential spatial modulation (G-DSM).

The optimal power allocation between the reference block and normal blocks studied and derived in [6], is implemented in the proposed GD-SM and G-DSM systems. The simulation results demonstrate that both GD-SM and G-DSM with optimal power allocation yield improved error performance as compared to the respective system, with equal power allocated to the reference and normal blocks. The error performance is also shown to approach that of the coherent SM detector of equal spectral efficiency, as the length of the transmitted frame increases.

The remainder of this paper is organized as follows. In Section II, we present the system models for coherent SM and DSM from [1] and [4-5], respectively. In Section III, we introduce the GD-SM scheme and present the optimal power allocation given by [6]. In Section IV, we extend the structure of GD-SM and optimal power allocation to G-DSM. The theoretical performance analysis and complexity analysis are presented in Section V and Section VI, respectively. Section VII presents the numerical results obtained from Monte-Carlo simulations, and Section VIII concludes the paper.

Notation: Bold lowercase and uppercase letters denote vectors and matrices, respectively. $(\cdot)^T$ and $\|\cdot\|_F$ are the transpose and the Frobenius norm of a vector or matrix. $\lfloor\cdot\rfloor$, $(\cdot)!$ and $(\cdot)!!$ are the floor operator, the factorial of an argument and the double factorial of an argument, respectively. $\boldsymbol{I}_N$ is the $N \times N$ identity matrix, $diag(\boldsymbol{x})$ is a square diagonal matrix with elements of the vector $\boldsymbol{x}$, and $E[\cdot]$ is the expected value of an argument.

2. System Model

2.1. Spatial Modulation [1]

Consider an SM system with N_t transmit antennas and N_r receive antennas. Information is transmitted via the antenna index as well as a modulated symbol. In each transmitted codeword, $\boldsymbol{x} \in \mathbb{C}^{N_t \times 1}$, only a single antenna is activated, while the remaining antennas transmit zero power. For each frame, $b_{SM1} = \log_2(N_t)$ bits determine the index, i ($i \in [1{:}N_t]$), of the activated transmit antenna, and $b_{SM2} = \log_2(M)$ bits determine the symbol, s, to be transmitted, which is drawn from the M-QAM or M-PSK constellation, $\boldsymbol{\chi}$, of normalized power, i.e. $E[|s|^2] = 1$. Therefore, the spectral efficiency of SM is $b_{SM1} + b_{SM2}$ bits/s/Hz.

The transmitted codeword is now $\boldsymbol{x} = [0, \dots, 0, s, 0, \dots, 0]^T$, where the i^{th} element is the only non-zero entry in $\boldsymbol{x}$. The received signal, $\boldsymbol{y} \in \mathbb{C}^{N_r \times 1}$, is then:

$$\boldsymbol{y} = \boldsymbol{H}\boldsymbol{x} + \boldsymbol{n}, \tag{A.1}$$

where $\boldsymbol{H} \in \mathbb{C}^{N_r \times N_t}$ and $\boldsymbol{n} \in \mathbb{C}^{N_r \times 1}$ denote the frequency flat Rayleigh fading channel matrix and the additive white Gaussian noise (AWGN) vector, respectively. The entries of $\boldsymbol{H}$ and $\boldsymbol{n}$ are independent and identically distributed (i.i.d.) complex random variables with Gaussian distributions $\mathcal{CN}(0,1)$ and $\mathcal{CN}(0, \sigma_{SM}^2)$, respectively. Therefore, the average SNR of the SM system is $\bar{\gamma}_{SM} = \frac{1}{\sigma_{SM}^2}$.

At the receiver, the joint detection rule based on the maximum likelihood (ML) principle may be employed to estimate the antenna index and transmitted symbol as [4]:

$$[\hat{\imath}, \hat{s}] = \underset{\substack{\forall \hat{\imath} \\ \forall \hat{s}}}{\operatorname{argmin}} \|\boldsymbol{y} - \boldsymbol{H}\hat{\boldsymbol{x}}\|_F^2 . \tag{A.2}$$

The ML detector utilizes the CSI to perform an exhaustive search over all antenna indices and M symbols to achieve optimal error performance.

2.2. Differential Spatial Modulation [4-5]

In DSM, communication is carried out block-wise, where one of Q antenna matrices (AMs) is selected to transmit N_t symbols, via N_t transmit antennas over N_t time slots. DSM maintains the property of SM whereby in each time slot only a single transmit antenna is activated, which is determined by the selected AM, while the remaining antennas transmit zero power.

There are a total of $Q = 2^{\lfloor \log_2(N_t!) \rfloor}$ unique AMs available for use, where each AM, $\boldsymbol{AM}_q$ ($q \in [1{:}\,Q]$), is an $N_t \times N_t$ matrix containing a single non-zero entry in each column (time slot). For example, given $N_t = 2$, $Q = 2$, and the set of AMs is given by $\boldsymbol{AM}_q = \begin{bmatrix} 1 & 0 \\ 0 & 1 \end{bmatrix}, \begin{bmatrix} 0 & 1 \\ 1 & 0 \end{bmatrix}$, of which $\boldsymbol{AM}_2 = \begin{bmatrix} 0 & 1 \\ 1 & 0 \end{bmatrix}$.

For the t^{th} transmitted space-time block, $b_{DSM1} = \log_2(Q)$ bits determine the index, q, of the AM to be used, and $b_{DSM2} = N_t \log_2(M)$ bits determine the modulated symbols, s_l ($l \in [1{:}\,N_t]$), which are drawn from the normalized M-PSK constellation, $\boldsymbol{\psi}$. The spectral efficiency of DSM therefore is $\frac{1}{N_t}(b_{DSM1} + b_{DSM2})$ bits/s/Hz [5]. The N_t modulated symbols constitute the symbol vector, $\boldsymbol{s}^{(t)} = [s_1, \dots, s_{N_t}]$.

Then, for the t^{th} space-time block, the information matrix, $\boldsymbol{S}^{(t)} \in \mathbb{C}^{N_t \times N_t}$, is given by:

$$\boldsymbol{S}^{(t)} = \boldsymbol{AM}_q diag\left(\boldsymbol{s}^{(t)}\right). \tag{A.3}$$

The differential transmission matrix, $\boldsymbol{X}^{(t)} \in \mathbb{C}^{N_t \times N_t}$, is then expressed as:

$$\boldsymbol{X}^{(t)} = \boldsymbol{X}^{(t-1)} \boldsymbol{S}^{(t)}, \tag{A.4}$$

where $\boldsymbol{X}^{(0)} = \boldsymbol{I}_{N_t}$. Note that for DSM, information is differentially encoded using the differential transmission matrix of the preceding space-time block. The received signal, $\boldsymbol{Y}^{(t)} \in \mathbb{C}^{N_r \times N_t}$, is calculated as follows:

$$\boldsymbol{Y}^{(t)} = \boldsymbol{H}^{(t)} \boldsymbol{X}^{(t)} + \boldsymbol{N}^{(t)}, \tag{A.5}$$

where $\boldsymbol{N}^{(t)} \in \mathbb{C}^{N_r \times N_t}$, is the AWGN matrix whose entries are i.i.d. random variables with Gaussian distribution $\mathcal{CN}(0, \sigma_{DSM}^2)$. The average SNR for the DSM system is therefore $\bar{\gamma}_{DSM} = \frac{1}{\sigma_{DSM}^2}$.

Assuming quasi-static fading, we have $\boldsymbol{H}^{(t)} = \boldsymbol{H}^{(t-1)}$, and using (A.4), the received signal $\boldsymbol{Y}^{(t)}$ may be rewritten as:

$$\boldsymbol{Y}^{(t)} = \boldsymbol{Y}^{(t-1)}\boldsymbol{S}^{(t)} + \widetilde{\boldsymbol{N}}^{(t)}, \tag{A.6}$$

where $\boldsymbol{Y}^{(t-1)} = \boldsymbol{H}^{(t-1)}\boldsymbol{X}^{(t-1)} + \boldsymbol{N}^{(t-1)}$ and $\widetilde{\boldsymbol{N}}^{(t)} = \boldsymbol{N}^{(t)} - \boldsymbol{N}^{(t-1)}\boldsymbol{S}^{(t)}$.

The ML detector may then be defined as [4]:

$$\left[\hat{q}, \hat{\boldsymbol{s}}^{(t)}\right] = \underset{\substack{\forall\, \hat{q} \\ \{\hat{s}_l \in \boldsymbol{\psi}\}_{l=1}^{N_t}}}{\operatorname{argmin}} \left\| \boldsymbol{Y}^{(t)} - \boldsymbol{Y}^{(t-1)}\widehat{\boldsymbol{S}}^{(t)} \right\|_F^2. \tag{A.7}$$

From (A.7), we note that estimation-detection is employed at the detector, since $\boldsymbol{Y}^{(t-1)}$ is used as an estimation of the channel in order to retrieve the information in $\boldsymbol{Y}^{(t)}$ [6]. Also, the current and preceding received signals are both transmitted at an average SNR of $\bar{\gamma}_{DSM}$.

3. A Generalized Differential Scheme for Spatial Modulation (GD-SM) with Optimal Power Allocation

In this section, we introduce a GD-SM system based on SM [1-2], wherein, similar to GDM [6-7], transmission power is allocated at different levels to the reference and normal codewords in order to improve the system error performance.

3.1. Proposed GD-SM Scheme

In GD-SM, each transmitted frame consists of $K = N_t + L$ codewords, of which the first N_t serve as reference codewords and convey no information, while the remaining L normal codewords transmit information. Each codeword transmits a single modulated symbol via one of the N_t transmit antennas, therefore the code rate for GD-SM is derived as $R = \frac{L}{K}$.

The reference codewords are transmitted over a duration of N_t time slots. Each transmit antenna is activated once and only once over the successive N_t reference time slots. As a result, we obtain a reference signal at the receiver from each of the N_t transmit antennas, which provides an estimate of the channel between the individual transmit antenna and the receive antennas. Thus, we may retrieve the information contained in the subsequent normal codewords using the reference signals.

Firstly, the differential reference codeword, $x_r = 1$, is transmitted via each transmit antenna over the first N_t time slots. Then the received reference signal during the l^{th} ($l \in [1: N_t]$) reference time slot, $\boldsymbol{y}_{rl} \in \mathbb{C}^{N_r \times 1}$, is calculated as:

$$\boldsymbol{y}_{rl} = \boldsymbol{h}_{rl} x_r + \boldsymbol{n}_{rl}, \tag{A.8}$$

where $\boldsymbol{h}_{rl} \in \mathbb{C}^{N_r \times 1}$ and $\boldsymbol{n}_{rl} \in \mathbb{C}^{N_r \times 1}$ are the l^{th} column vectors of the channel fading matrix, $\boldsymbol{H}_r \in \mathbb{C}^{N_r \times N_t}$, and the AWGN matrix, $\boldsymbol{N}_r \in \mathbb{C}^{N_r \times N_t}$, respectively. The entries of $\boldsymbol{H}_r$ and $\boldsymbol{N}_r$ are i.i.d. complex random variables with Gaussian distributions $\mathcal{CN}(0,1)$ and $\mathcal{CN}(0, \sigma_r^2)$, respectively. Therefore, the average SNR at which the reference codewords are transmitted is $\bar{\gamma}_r = \frac{1}{\sigma_r^2}$.

Information is then transmitted via the remaining L normal codewords. For the t^{th} time slot ($t \in [1: L]$), $\log_2(N_t)$ bits determine the index, j, of the antenna to be activated, and $\log_2(M)$ bits determine the modulated symbol, s, which is drawn from either an M-PSK or M-QAM constellation, $\boldsymbol{\Omega}$, of normalized power, i.e. $E[|s|^2] = 1$. We note that GD-SM achieves the same spectral efficiency as that of coherent SM. The codeword, $\boldsymbol{s}^{(t)} \in \mathbb{C}^{N_t \times 1}$, transmitted in the t^{th} time slot is $\boldsymbol{s}^{(t)} = [0, \dots, s, \dots, 0]^T$, where the j^{th} element is the only non-zero entry in $\boldsymbol{s}^{(t)}$.

With this, the differentially encoded vector for the normal codewords is given by

$$\boldsymbol{x}_n^{(t)} = x_r \boldsymbol{s}^{(t)}. \tag{A.9}$$

From (A.9), it is obvious that $\boldsymbol{x}_n^{(t)} = \boldsymbol{s}^{(t)}$, since $x_r = 1$. This is advantageous as it permits the use of either an M-PSK or M-QAM normalized constellation in the system. Thus the error performance may be improved for large M by simply using the power-efficient QAM constellation [8].

The received signal, $\boldsymbol{y}^{(t)} \in \mathbb{C}^{N_r \times 1}$, is then calculated as:

$$\boldsymbol{y}^{(t)} = \boldsymbol{H}^{(t)}\boldsymbol{x}_n^{(t)} + \boldsymbol{n}^{(t)}, \tag{A.10}$$

where $\boldsymbol{H}^{(t)} \in \mathbb{C}^{N_r \times N_t}$ is the channel fading matrix and $\boldsymbol{n}^{(t)} \in \mathbb{C}^{N_r \times 1}$ is the AWGN vector, whose entries are i.i.d. complex random variables with Gaussian distributions $\mathcal{CN}(0,1)$ and $\mathcal{CN}(0, \sigma_n^2)$, respectively. The average SNR for the normal codewords is therefore $\bar{\gamma}_n = \frac{1}{\sigma_n^2}$.

Given that the j^{th} transmit antenna is activated, the received signal may be also represented as:

$$\boldsymbol{y}^{(t)} = \boldsymbol{h}_j^{(t)} x_n^{(t)} + \boldsymbol{n}^{(t)}, \tag{A.11}$$

where $\boldsymbol{h}_j^{(t)} \in \mathbb{C}^{N_r \times 1}$ is the j^{th}column vector of $\boldsymbol{H}^{(t)}$ and $x_n^{(t)} = x_r s$, respectively.

Assuming quasi-static fading, where the channel fading matrix remains constant for the duration of the frame, i.e. $\boldsymbol{H}_r = \boldsymbol{H}^{(t)}$; we may rewrite the received signal in (A.11) as:

$$\boldsymbol{y}^{(t)} = \boldsymbol{y}_{rj} s + \boldsymbol{n}^{(t)} - \boldsymbol{n}_{rj} s. \tag{A.12}$$

The ML detector is then employed for GD-SM and is derived similar to (A.7) as:

$$[\hat{\jmath}, \hat{s}] = \underset{\substack{\forall\, \hat{\jmath} \\ \forall\, \hat{s}}}{\operatorname{argmin}} \left\| \boldsymbol{y}^{(t)} - \boldsymbol{y}_{r\hat{\jmath}} \hat{s} \right\|_F^2. \tag{A.13}$$

From (A.13), it is clear that estimation-detection [6] is used, whereby the reference signals, $\boldsymbol{y}_{rl}$ ($l \in [1{:}\, N_t]$), provide an estimate of the channel between the l^{th} transmit antenna and the N_r receive antennas, which is utilized to recover the information contained in $\boldsymbol{y}^{(t)}$. Therefore, by determining which received reference signal and modulated symbol combination minimizes the metric in (A.13), we may estimate the activated transmit antenna and modulated symbol transmitted in the t^{th} time slot. The ML detector performs an exhaustive search over MN_t unique combinations during each time slot.

3.2. Optimal Power Allocation for the Proposed GD-SM Scheme

The objective of optimal power allocation is to transmit the reference codeword with a higher power than the normal codewords ($\bar{\gamma}_r > \bar{\gamma}_n$) and to maximize the average output SNR.

In [6-7], the GDM schemes allocate more transmit power to the reference blocks than the normal blocks allowing for improved performance through estimation-detection at the receiver. Both schemes assume that a transmitted frame of length P blocks comprises of one reference block and $(P-1)$ normal blocks. An optimization problem to constrain the average transmit power, $\bar{\gamma}$, is then formulated as [6-7]:

$$\bar{\gamma}_r + (P-1)\bar{\gamma}_n = P\bar{\gamma}. \tag{A.14}$$

The optimal solutions to (A.14) are obtained by using the Lagrange multiplier method, however unlike [6], the solution given in [7] to maximize the output SNR is dependent upon the statistics of the system. Therefore, we employ the optimal power allocation from [6] in GD-SM.

From [6], the optimal power allocation between the reference and normal blocks is given by:

$$\bar{\gamma}_r = \frac{P\bar{\gamma}}{1+\sqrt{P-1}}\,, \tag{A.15}$$

$$\bar{\gamma}_n = \frac{P\bar{\gamma}}{\sqrt{P-1}+P-1}, \tag{A.16}$$

respectively. Note that the power allocation is independent of the number of transmit and receive antennas [6].

From (A.12), it is obvious that the received signal in the t^{th} time slot consists of two noise components, each with a different variance. Furthermore, the optimization problem in (A.14) constrains the average SNR of the system using transmit power for the reference and normal blocks. As such, we define the equivalent coherent noise variance of the system as:

$$\sigma_{eq}^2 = \frac{\sigma_r^2 + \sigma_n^2}{2}\,, \tag{A.17}$$

where $\sigma_r^2 = \frac{1+\sqrt{P-1}}{P\bar{\gamma}}$ and $\sigma_n^2 = \frac{\sqrt{P-1}+P-1}{P\bar{\gamma}}$ are derived from (A.15) and (A.16), respectively.

Following (A.17), the equivalent coherent SNR of the system, $\bar{\gamma}_{eq} = \frac{1}{\sigma_{eq}^2}$, is then given by:

$$\bar{\gamma}_{eq} = \left[\frac{2P}{2\sqrt{P-1}+P}\right]\bar{\gamma}\,. \tag{A.18}$$

From (A.18), we note that when $P = 2$, the system performs as a conventional differential modulation system, i.e. equal power is allocated to all blocks within the frame.

In GD-SM, a frame of length K codewords consists of N_t reference codewords and $L = K - N_t$ normal codewords. In order to apply the power allocation given in [6] (which comprises of one reference block and $(P-1)$ normal blocks) to GD-SM, we let N_t codewords constitute a single block. Therefore, each frame now comprises of $\frac{K}{N_t}$ blocks, of which the first block is the reference block and the remaining $\frac{L}{N_t} = \frac{K}{N_t} - 1$ blocks are the normal blocks. With this, the average SNR for the reference and normal codewords, and the equivalent coherent SNR for GD-SM are given by (A.15), (A.16) and (A.18), respectively, with $P = \frac{K}{N_t}$.

4. Extension of Optimal Power Allocation to Generalized DSM (G-DSM)

In this section, we extend the frame structure and power allocation concept used in GD-SM to the current DSM [4-5] architecture (Section 2.2). In generalized differential spatial modulation (G-DSM), each frame comprises of $K = 1 + L$ space-time blocks, of which the first block is the reference block (containing no information) and is transmitted at a higher power than the subsequent L normal blocks. As in DSM, each space-time block selects one of Q AMs to transmit N_t symbols over N_t time slots. Therefore, the code rate for G-DSM is derived as $R = \frac{L}{K}$.

In the reference block, the differentially encoded reference matrix is given by $\boldsymbol{X}_r = \boldsymbol{I}_{N_t}$. The received signal in the reference (first) block is then given by:

$$\boldsymbol{Y}_r = \boldsymbol{H}_r\boldsymbol{X}_r + \boldsymbol{N}_r, \tag{A.19}$$

where $\boldsymbol{H}_r \in \mathbb{C}^{N_r \times N_t}$ and $\boldsymbol{N}_r \in \mathbb{C}^{N_r \times N_t}$ are the channel fading matrix and AWGN matrix in the reference block whose entries are i.i.d. complex random variables with Gaussian distributions $\mathcal{CN}(0,1)$ and $\mathcal{CN}(0, \sigma_r^2)$, respectively. The average SNR at which the reference block is transmitted is therefore $\bar{\gamma}_r = \frac{1}{\sigma_r^2}$.

The remaining L normal blocks in the frame convey information; $\log_2(Q)$ bits determine the index, q, of the AM and $N_t \log_2(M)$ bits determine the symbols, $s_l \in \boldsymbol{\Omega}$ ($l \in [1: N_t]$), which constitute the symbol vector, $\boldsymbol{s}_n$. For the t^{th} ($t \in [1: L]$) space-time block, the information matrix given by $\boldsymbol{S}^{(t)} = \boldsymbol{A}\boldsymbol{M}_q diag(\boldsymbol{s}_n)$ is differentially encoded using $\boldsymbol{X}_r$ as:

$$\boldsymbol{X}_n^{(t)} = \boldsymbol{X}_r \boldsymbol{S}^{(t)}. \tag{A.20}$$

Again, we note that since $\boldsymbol{X}_r$ is the identity matrix, $\boldsymbol{X}_n^{(t)} = \boldsymbol{S}^{(t)}$ and as such, the symbols constituting $\boldsymbol{s}_n$ may be drawn from a PSK or power-efficient QAM constellation, which is not possible in [3-5].

The received signal in the t^{th} normal block is then expressed as:

$$\boldsymbol{Y}^{(t)} = \boldsymbol{H}^{(t)} \boldsymbol{X}_n^{(t)} + \boldsymbol{N}^{(t)}, \tag{A.21}$$

where $\boldsymbol{N}^{(t)} \in \mathbb{C}^{N_r \times N_t}$ is the normal block AWGN matrix whose entries are i.i.d. complex random variables with Gaussian distribution $\mathcal{CN}(0, \sigma_n^2)$. The average SNR for the t^{th} normal block may be written as $\bar{\gamma}_n = \frac{1}{\sigma_n^2}$.

Assuming quasi-static fading where $\boldsymbol{H}_r = \boldsymbol{H}^{(t)}$, $\boldsymbol{Y}^{(t)}$ may be rewritten as:

$$\boldsymbol{Y}^{(t)} = \boldsymbol{Y}_r \boldsymbol{S}^{(t)} + \boldsymbol{N}^{(t)} - \boldsymbol{N}_r \boldsymbol{S}^{(t)}. \tag{A.22}$$

The ML detector may then be defined as:

$$[\hat{q}, \hat{\boldsymbol{s}}_n] = \underset{\substack{\forall\, \hat{q} \\ \{\hat{s}_l \in \boldsymbol{\Omega}\}_{l=1}^{N_t}}}{\operatorname{argmin}} \left\| \boldsymbol{Y}^{(t)} - \boldsymbol{Y}_r \widehat{\boldsymbol{S}}^{(t)} \right\|_F^2. \tag{A.23}$$

Once more, the reference signal, $\boldsymbol{Y}_r$, is used to estimate the channel and recover the information in $\boldsymbol{Y}^{(t)}$. The ML detector performs an exhaustive search through QM^{N_t} combinations for each normal block.

For G-DSM, given $P = K$, the transmit power is allocated between the reference and normal blocks according to (A.15) and (A.16), and the maximized equivalent coherent SNR of the system given by (A.18).

5. Asymptotic Performance Analysis

An asymptotic upper bound on the average bit error probability (ABEP) for GD-SM and G-DSM is derived for PSK and QAM modulation, based on the derivation given for high-rate amplitude-PSK (APSK) DSM in [9].

The ABEP for GD-SM is union bounded by [9-10]:

$$P_{ABEP} \leq \sum_{\boldsymbol{s}^{(t)} \in \boldsymbol{\Theta}} \sum_{\hat{\boldsymbol{s}}^{(t)} \in \boldsymbol{\Theta}} \frac{N\left(\boldsymbol{s}^{(t)}, \hat{\boldsymbol{s}}^{(t)}\right) P\left(\boldsymbol{s}^{(t)} \to \acute{\boldsymbol{s}}^{(t)}\right)}{b 2^b}, \tag{A.24}$$

where b is the total number of bits conveyed in a single codeword, $P\left(\boldsymbol{s}^{(t)} \to \acute{\boldsymbol{s}}^{(t)}\right)$ is the pairwise error probability (PEP) of choosing codeword $\acute{\boldsymbol{s}}^{(t)}$ given that codeword $\boldsymbol{s}^{(t)}$ was transmitted, $N\left(\boldsymbol{s}^{(t)}, \acute{\boldsymbol{s}}^{(t)}\right)$ is the total number of bits in error between codewords $\boldsymbol{s}^{(t)}$ and $\acute{\boldsymbol{s}}^{(t)}$, and $\boldsymbol{\Theta}$ is the set of all legitimate codewords. Note that the codeword $\boldsymbol{s}^{(t)} \in \mathbb{C}^{N_t \times 1}$ is given (from Section 3.1.) as $\boldsymbol{s}^{(t)} = [0, \dots, s, \dots, 0]^T$, where s is drawn from either an M-PSK or an M-QAM constellation of normalized power, and whose position in $\boldsymbol{s}^{(t)}$ represents the index of the active transmit antenna.

From [9], we have, $\boldsymbol{\Delta} = \boldsymbol{s}^{(t)} - \acute{\boldsymbol{s}}^{(t)} = \left[\boldsymbol{\Upsilon}_1, \dots, \boldsymbol{\Upsilon}_{N_t}\right]^T$, where $\boldsymbol{\Upsilon}_i$ ($i \in [1{:}\, N_t]$) denotes the i^{th} row of $\boldsymbol{\Delta}$. The number of non-zero rows in $\boldsymbol{\Delta}$ is then denoted by κ, and the corresponding indices of the non-zero rows is $\{v_i\}_{i=1}^{\kappa}$. Then, using the maximized equivalent coherent SNR for GD-SM given by (A.18) with $P = \frac{K}{N_t}$, the PEP is bounded by [9]:

$$P\left(\boldsymbol{s}^{(t)} \to \hat{\boldsymbol{s}}^{(t)}\right) \leq \left(\frac{1}{\bar{\gamma}_{eq}}\right)^{\kappa N_r} \frac{8^{\kappa N_r}(2\kappa N_r - 1)!!}{2\left(\left\|\boldsymbol{\Upsilon}_{v_i}\right\|_F^2 \cdots \left\|\boldsymbol{\Upsilon}_{v_\kappa}\right\|_F^2\right)^{N_r}(2\kappa N_r)!!}. \tag{A.25}$$

The asymptotic upper bound of the ABEP for G-DSM is also given by (A.24) and (A.25), with the only exceptions being $\boldsymbol{\Delta} = \boldsymbol{S}^{(t)} - \hat{\boldsymbol{S}}^{(t)} = \left[\boldsymbol{\Upsilon}_1, \ldots, \boldsymbol{\Upsilon}_{N_t}\right]^T$ given that the information matrix $\boldsymbol{S}^{(t)}$ was transmitted and $\hat{\boldsymbol{S}}^{(t)}$ was estimated at the receiver, $\boldsymbol{\Theta}$ is the set of all legitimate information matrices, and the maximized $\bar{\gamma}_{eq}$ is given by (A.18) with $P = K$. Note that for G-DSM, the information matrix $\boldsymbol{S}^{(t)}$ is given (from Section 4.) as $\boldsymbol{S}^{(t)} = \boldsymbol{A}\boldsymbol{M}_q diag(\boldsymbol{s}_n)$, where $\boldsymbol{s}_n$ is the symbol vector comprising of N_t symbols, which are drawn from either an M-PSK or an M-QAM constellation of normalized power.

Note, when $\bar{\gamma}_{eq} = \bar{\gamma}$, i.e. P is set to 2 in (A.18), the upper bound given by (A.24) is for the specific system with equal power allocated between the reference and normal codewords/blocks.

6. Complexity Analysis

In this section, we analyze and present the computational complexity of the ML detectors for SM, DSM, GD-SM and G-DSM, for a complete frame. We use the concept of computational complexity from [11], which indicates the total number of real-valued multiplications incurred in an algorithm. Note, multiplication of 2 complex arguments results in a total of 4 real-valued multiplications.

6.1. SM

In SM, we assume that a frame consists of a single codeword. Then:

1. In each frame, the ML detector first computes $\boldsymbol{H}\hat{\boldsymbol{x}}$, where $\hat{\boldsymbol{x}}$ is a column vector containing a single non-zero entry. This computation results in a total of $4N_r$ real-valued multiplications.
2. The subtraction operation in $\boldsymbol{y} - \boldsymbol{H}\hat{\boldsymbol{x}}$ requires no real-valued multiplications.
3. Computing the Frobenius norm requires a further $2N_r$ real-valued multiplications.

The ML detector searches through a total of MN_t different combinations for SM, therefore the total computational complexity for each frame in SM is $C_{SM} = 6N_rN_tM$ real-valued multiplications.

6.2. DSM

We assume that the frame length in DSM is L space-time blocks. The computational complexity incurred during a single space-time block for DSM is given in [11]. Using this, the total computational complexity for the DSM ML detector for the duration of a frame is $C_{DSM} = 6N_r N_t Q M^{N_t} L$ real-valued multiplications.

6.3. GD-SM

Assuming a search space of $N_t M$ and L normal (information conveying) codewords, we have the following.

1. Firstly, computing $\boldsymbol{y}_{r\hat{j}}\hat{s}$, for a single symbol and received reference signal, requires $4N_r$ real-valued multiplications. Since $\boldsymbol{y}_{r\hat{j}}$ does not change for the duration of the frame, this computation need only take place once for the entire frame and may be stored for later use. Therefore, this computation will require a total of $4N_r N_t M$ real-valued multiplications for the entire frame.
2. The Frobenius norm requires 2 real-valued multiplications for each entry in the column vector obtained after the subtraction operation. Therefore, a total of $2N_r N_t ML$ real-valued multiplications is incurred for the duration of the frame.

The total computational complexity for the GD-SM ML detector is therefore, $C_{GD-SM} = 4N_r N_t M + 2N_r N_t ML$ real-valued multiplications.

6.4. G-DSM

Given a search space of QM^{N_t} and L normal (information conveying) blocks, we have:

1. Computing $\boldsymbol{Y}_r\widehat{\boldsymbol{S}}$ for all $\hat{q}$ and $\hat{s}_l$ in a single space-time block requires $4N_r N_t Q M^{N_t}$ real-valued multiplications. However, since $\boldsymbol{Y}_r$ remains constant for the duration of the frame, this computation need only be executed once and may be stored for use in the remaining blocks of the frame.
2. The Frobenius norm requires a further $2N_r N_t Q M^{N_t} L$ real-valued multiplications in each frame.

Thus the total computational complexity for the G-DSM ML detector is $C_{G-DSM} = 4N_r N_t Q M^{N_t} + 2N_r N_t Q M^{N_t} L$ real-valued multiplications.

Assuming a DSM frame length of L blocks and a G-DSM frame consisting of L normal blocks, we note that the computational complexity of the G-DSM ML detector is lower than that of the conventional DSM ML detector. The percentage reduction may be expressed as:

$$\%\, Reduction \;= \frac{100(C_{DSM} - C_{G-DSM})}{C_{DSM}} = \frac{400L - 400}{6L}. \tag{A.26}$$

As $L \to \infty$, the percentage reduction approaches a maximum of 66.67%. Nonetheless, for a frame length of only $L = 100$, a substantial computational complexity reduction of 66% is achieved over the DSM ML detector. Note that the achieved reduction is independent of M, Q, N_r and N_t.

7. Numerical Results

In this section, Monte-Carlo simulation results for GD-SM and coherent SM, using PSK and QAM constellations, are compared. Furthermore, we demonstrate the error performance improvement achieved by G-DSM relative to conventional DSM and coherent SM, with systems of equivalent spectral efficiency, using PSK and QAM constellations. We simulate the results for frame lengths of $K = 100$ and $K = 400$, and since N_r has no effect on the power allocation for the system, we choose $N_r = 2$. The simulated BER and the theoretical upper bound given by (A.24), as discussed in detail in Section 5, is plotted against the average SNR $\bar{\gamma}$ (dB) for the schemes.

It is clear from Figure A.1 and Figure A.2 that the conventional GD-SM scheme (where $\bar{\gamma}_r = \bar{\gamma}_n = \bar{\gamma}$) suffers from an approximate 3 dB performance penalty when compared to the coherent detection of SM. In Figure A.1, the proposed GD-SM scheme with optimal power allocation and $K = 100$ achieves a gain of 1.6 dB over the conventional GD-SM scheme, while using a frame length of 400 achieves an additional gain of 0.7 dB, bringing it within 0.6 dB of coherent SM. We note in Figure A.2 that increasing N_t has a minimal effect on the error performance, as GD-SM with $K = 400$ is within 0.5 dB of SM down to a bit error rate (BER) of 10^{-5}. We also note that the theoretical upper bound is tight for both frame lengths in Figure A.1 and Figure A.2, down to a BER of 10^{-5}.

Figure A.3 demonstrates that GD-SM with 64-QAM modulation and a frame length of 400 attains a gain of approximately 2.6 dB over the conventional GD-SM scheme, and achieves near coherent error performance for majority of the SNR range (within 0.4 dB of SM).

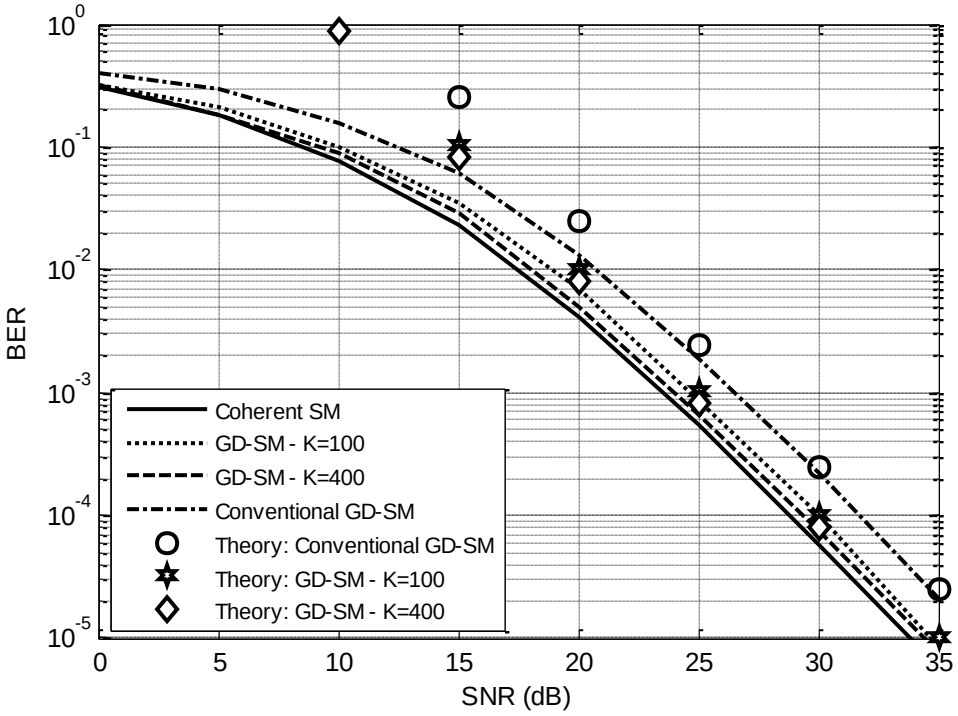

Figure A.1: 16-PSK BER Performance comparison with $N_t = 2$.

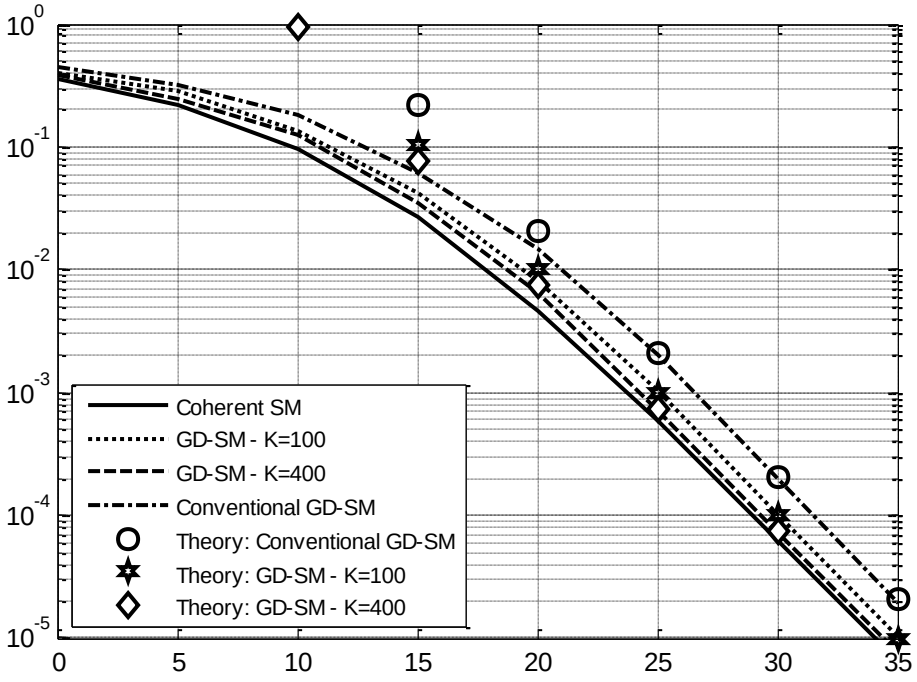

Figure A.2: 16-PSK BER Performance comparison with $N_t = 4$.

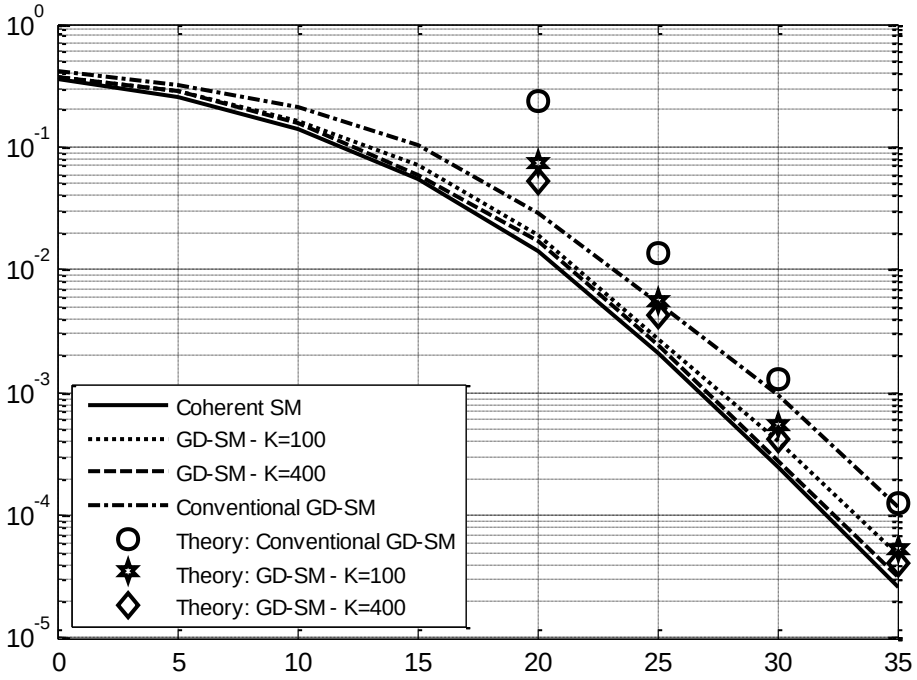

Figure A.3: 64-QAM BER Performance comparison with $N_t = 2$.

In Figure A.4, we observe that for a 16-PSK and 5 bits/s/Hz transmission, G-DSM considerably outperforms conventional DSM and achieves near coherent performance for both frame lengths. This is achieved despite the fact that G-DSM requires 4 transmit antenna as opposed to 2 for SM in order to achieve the same spectral efficiency. For a frame length of 400, G-DSM is within 0.3 dB of the error performance of the coherent detector at high SNR, while G-DSM with $K = 100$ is a further 0.4 dB away and demonstrates a gain of 2 dB when compared to conventional DSM.

In Figure A.5, it is demonstrated that G-DSM with PSK modulation achieves a gain of 2.5 dB over conventional DSM. Furthermore, the structure of G-DSM, advantageously, allows the use of QAM modulation to improve error performance, and it is shown to achieve a gain of approximately 5.5 dB over conventional DSM, which is limited to only PSK constellations.

The results obtained demonstrate theoretically and via simulations that the error performance is improved as the frame length increases. However, although a large frame length is ideal to mitigate the 3 dB error performance loss experienced due to differential modulation, it is important to be mindful when selecting the length of the frame, as this will in turn affect the peak power required for the reference block [6].

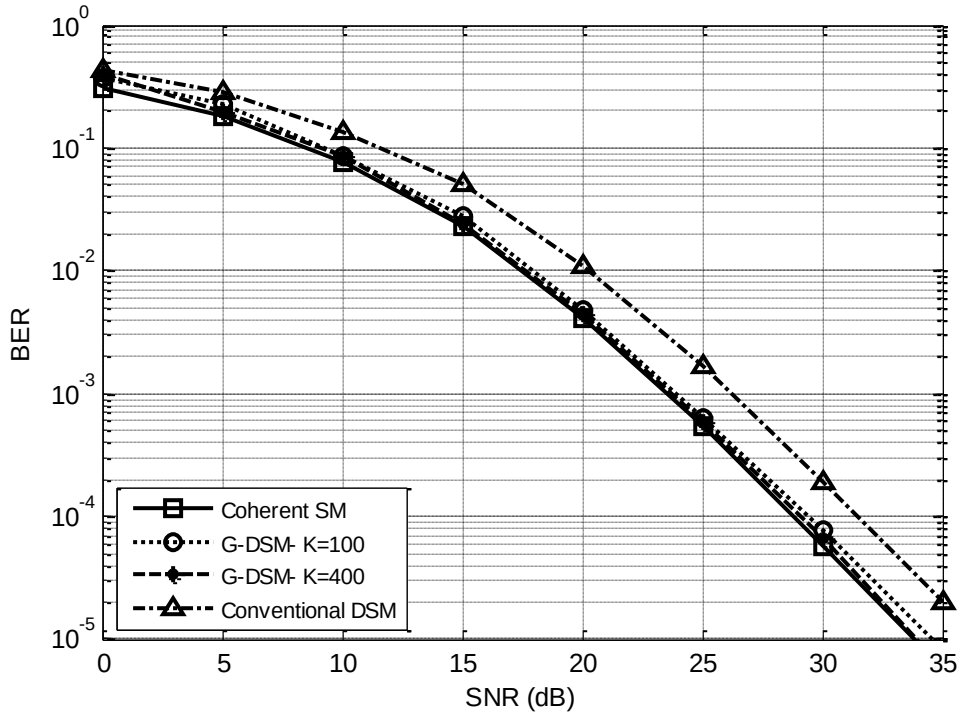

Figure A.4: 16-PSK BER Performance comparison for the case of 5 bits/s/Hz transmission.

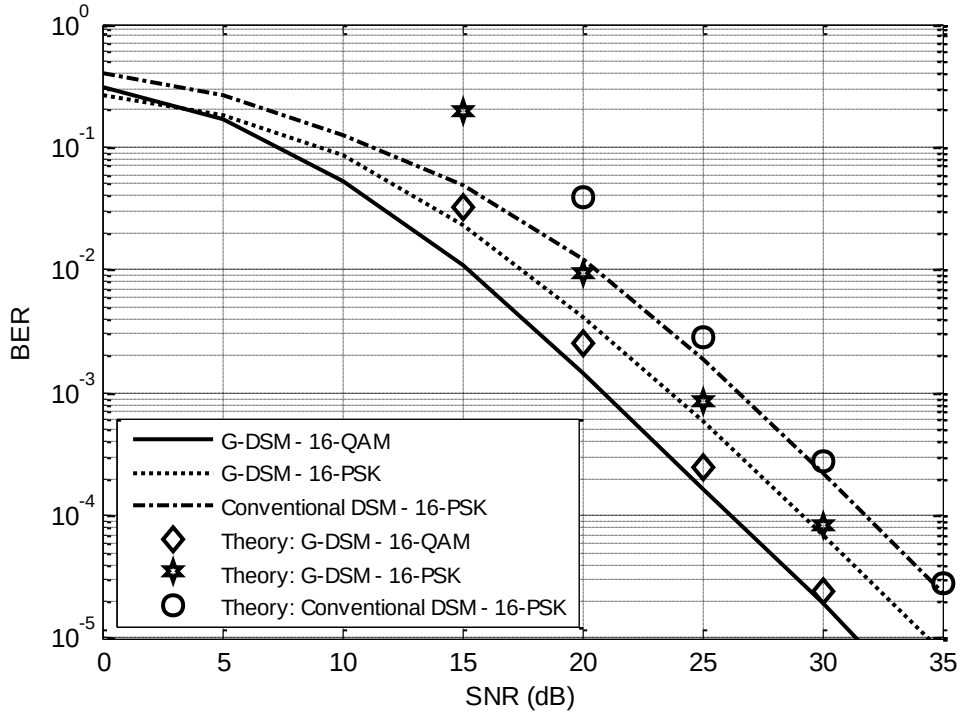

Figure A.5: G-DSM BER Performance comparison with $K = 400$, and $N_t = 2$.

8. Conclusion

In this paper, we proposed a GD-SM system, which employs optimal power allocation to improve error performance. Furthermore, the structure of GD-SM and the power allocation scheme is extended to conventional DSM in order to reduce the error performance penalty incurred compared to coherent SM. Both GD-SM and G-DSM use a frame structure comprising of a reference block against which numerous normal blocks are differentially encoded and decoded. By allocating more power to the reference block than the normal blocks, the received reference signal provides an enhanced estimation of the channel. These reference signals are utilized to recover the information in the normal blocks via estimation-detection. As a result, the error performance for a given average system SNR is improved. Simulation and theoretical results for GD-SM and G-DSM confirm that the error performance may approach that of the coherent detector when a large frame length is used. Furthermore, unlike conventional DSM, the architecture of GD-SM and G-DSM permit the use of M-QAM constellations to provide a marked improvement in error performance when M is large.

References

[1] R. Y. Mesleh, H. Haas, S. Sinanovic, C. W. Ahn, and S. Yun, "Spatial Modulation," *IEEE Trans. Veh. Tech.,* vol. 57, no. 4, pp. 2228 – 2241, Jul. 2008.

[2] R. Y. Mesleh, H. Haas, C. W. Ahn, and S. Yun, "Spatial Modulation – A New Low Complexity Spectral Efficiency Enhancing Technique," *in Proc. of the Conf. on Commun. and Netw., China*, pp. 1 – 5, Oct. 2006.

[3] N. Ishikawa, and S. Sugiura, "Unified Differential Spatial Modulation," *IEEE Wireless Commun. Lett.,* vol. 3, no. 4, pp. 337 – 340, Aug. 2014.

[4] Y. Bian, M. Wen, X. Cheng, H. V. Poor, and B. Jiao, "A Differential Scheme for Spatial Modulation," *in Proc. 2013 IEEE GLOBECOM,* pp. 3925 – 3930, Dec. 2013.

[5] Y. Bian, X. Cheng, M. Wen, L. Yang, H. V. Poor, and B. Jiao, "Differential Spatial Modulation," *IEEE Trans. Veh. Technol.,* vol. 64, no. 7, pp. 3262 – 3268, Jul. 2015.

[6] L. Li, Z. Fang, Y. Zhu, and Z. Wang, "Generalized Differential Transmission for STBC Systems," *in Proc. 2008 IEEE GLOBECOM,* pp. 1 – 5, Dec. 2008.

[7] Z. Fang, L. Li, X. Bao, and Z. Wang, "Generalized Differential Modulation for Amplify-and-Forward Wireless Relay Networks," *IEEE Trans. Veh. Tech.,* vol. 58, no. 6, pp. 3058 – 3062, Jul. 2009.

[8] A. Goldsmith, *Wireless Communications,* Cambridge University Press, 2005.

[9] J. Liu, L. Dan, P. Yang, L. Xiao, F. Yu, and Y. Xiao, "High-rate APSK-aided Differential Spatial Modulation: Design Method and Performance Analysis," *IEEE Commun. Lett.,* (early access), Sep. 2016.

[10] J.G. Proakis, *Digital Communications*, (4th ed.) New York: McGraw-Hill, pp. 263 – 264, 2001.

[11] L. Xiao, P. Yang, X. Lei, Y. Xiao, S. Fan, S. Li, and W. Xiang, "A Low-Complexity Detection Scheme for Differential Spatial Modulation," *IEEE Commun. Lett.,* vol. 19, no. 9, pp. 1516 – 1519, Sep. 2015.

Paper B: A Simple Low-Complexity Near-ML Detection Scheme for Differential Spatial Modulation

H. Xu, K. Kadathlal, and N. Pillay

Submitted to:

SAIEE Africa Research Journal, Currently under review

Abstract

Spatial modulation (SM) is an emerging transmission scheme which employs active transmit antenna indices and modulated signals to convey information. By nature, its detection is coherent, thereby requiring the channel state information (CSI) at the receiver in order to achieve optimal error performance. Compared to SM, differential spatial modulation (DSM) does not require the CSI at the receiver. However, the optimal maximum likelihood (ML) detection of DSM induces excessive computational complexity when the number of transmit antennas is large. In this paper, a simple low-complexity near-ML detection scheme is proposed for DSM, using M-ary phase shift keying (M-PSK) and M-M amplitude phase shift keying (M-M APSK) modulation. The proposed simple detection is based on the features of the PSK constellation and is shown to be independent of the constellation size, for DSM with either M-PSK or M-M APSK modulation. Simulation results demonstrate that for M-PSK and M-M APSK modulation, the proposed simple detection scheme achieves the same error performance as ML detection down to a bit error rate of 10^{-5}, with at least 98% reduction in computational complexity.

1. Introduction

Spatial modulation (SM) is an efficient transmission technique utilizing multiple-input multiple-output (MIMO) technology [1-3]. The difference between SM and conventional MIMO systems is that at any time instant, only one transmit antenna is activated to convey information, while the remaining antennas transmit zero power [1-3]. As a result, unlike conventional MIMO systems, SM requires no inter-antenna synchronization (IAS) at the transmitter and completely avoids inter-channel interference (ICI) at the receiver, while achieving a relatively high spectral efficiency, through use of only a single radio frequency chain [2-3]. The improved spectral efficiency is achieved by mapping the information bits to a constellation point (signal domain) and a specific transmit antenna index (spatial domain), which determine the amplitude and/or phase modulated (APM) symbol and the active transmit antenna, respectively. In order to achieve optimal error performance, SM performs coherent detection, which requires that the receiver has full knowledge of the channel state information (CSI). The result is increased complexity at the receiver as well as limitations imposed by pilot overhead and channel estimation errors [4]. To overcome these issues, various non-coherent, differentially encoded SM schemes have been developed [4-7].

Differential spatial modulation (DSM) [5-7] is a promising alternative to SM as its receiver does not require the CSI to perform detection. DSM maintains the merits of the SM system over conventional MIMO systems. However, it suffers from a 3 dB error performance penalty compared to SM, which is attributed to the non-coherent detection process [5, 7]. In DSM, communication is carried out block-wise; given N_t transmit antennas, one out of a maximum of Q antenna matrices (AMs) is selected, which determines the activation order of the N_t transmit antennas over N_t time slots. Thereafter, based on the selected AM, the N_t transmit antennas convey N_t APM symbols within the N_t time slots. Thus, similarly to SM, information bits are mapped to the N_t APM symbols and a specific AM.

The DSM schemes given in [5-7], draw the APM symbols from a M-ary phase shift keying (M-PSK) constellation. In [8], Martin extends the DSM scheme in [5] to a M-M amplitude phase shift keying (M-M APSK) constellation, which comprises of two M-PSK constellations with different amplitude levels. The proposed DSM system in [8] offers an improved spectral efficiency over DSM using M-PSK modulation. This is achieved by either transmitting the N_t symbols at a constant amplitude level, or by changing the amplitude level for each of the N_t symbols, during each transmission.

In order to achieve optimal error performance, the DSM receiver employs maximum likelihood (ML) detection, which is performed on a block-by-block basis. In each space-time block, the ML detector jointly estimates the AM index and the N_t APM symbols conveyed during transmission.

Therefore, the ML detector performs an exhaustive search over all possible combinations of AMs and APM symbols conveyed from each transmit antenna. Consequently, the complexity of the ML detection grows exponentially with an increase in the number of transmit antennas and M. In order to reduce this effect, low-complexity detection schemes have been proposed in [9] and [10], whose computational complexities are lower than that of ML detection.

The low-complexity detection scheme proposed in [9] operates on a symbol-by-symbol basis and uses the hard-limiter based ML (HL-ML) detection [11] to estimate the antenna index (AI) and the modulated PSK symbol in each time slot of each space-time block. If the estimated antenna indices form a legitimate AM, then the estimated AM and N_t PSK symbols are taken as the final output; otherwise the P most probable AMs are chosen for further search [9]. The complexity of the detection is shown to be independent of M, however, in order to achieve optimal error performance at a low signal-to-noise ratio (SNR), the detector is required to search through all, Q, AMs. This results in a complexity increase, as N_t increases.

Furthermore, in [10], a suboptimal low-complexity detector based on the ML criterion, is proposed for DSM. The symmetric property of the PSK constellation is exploited in the detection scheme and as a result approximately one-eighth of the signals are used to estimate the modulated symbols. Once completed, AM estimation is carried out, which takes into account more than Q AMs so as to facilitate low-complexity detection via the use of a Viterbi-like algorithm [10], when N_t is large. This, however, induces a minimal error performance penalty with respect to the ML detector, since the detector may estimate an AM which is not included in the legitimate Q AMs permitted for use during transmission [10]. Furthermore, the complexity of the detection is shown to be dependent upon M.

Motivated by the above, we propose another low-complexity near-ML detection scheme for DSM, whose complexity is independent of M and Q. The proposed detection scheme is simple and the complexity is even lower compared to those in [9] and [10]. The detector operates by first estimating the transmitted symbols, which are drawn from a PSK constellation (either M-PSK or M-M APSK), for the space-time block. This is accomplished by exploiting the fact that each received signal is a complex argument, each with an associated magnitude and phase. Thus, the proposed detection scheme focuses on the phase of the received signal and uses this information to estimate the symbol, from the employed PSK constellation, whose phase is nearest to that of the received signal. This significantly reduces the complexity of the detector, since an exhaustive search through the M constellation points is not required to estimate the transmitted symbols. Thereafter, the estimated symbols are utilized to determine the antenna activation order, which is determined in a similar manner to [10]. However, unlike [10], only Q AMs are involved in the calculation, since the proposed detection scheme does not make use of a Viterbi-like algorithm.

Thus, the estimated AM will always be one of the permitted Q AMs, and as such, the proposed detector will not suffer from a similar error performance penalty incurred in [10], relative to the ML detector.

The remainder of this paper is organized as follows. Section 2 gives the system model of DSM with M-PSK and M-M APSK constellations. Section 3 presents the current low-complexity detectors designed for DSM. In Section 4, we propose a near-ML low-complexity detector for DSM using an M-PSK constellation. Furthermore, we extend the detection algorithm to DSM using an M-M APSK constellation. The complexity of the proposed detectors are analyzed and compared to the ML detector and current low-complexity detectors, in Section 5. In Section 6, we discuss the simulation results of the detectors for different system configurations. Finally, Section 7 concludes the paper.

Notation: Bold lowercase and uppercase letters denote vectors and matrices, respectively. The $(i,j)^{th}$ entry of matrix $\boldsymbol{X}$ is denoted by $X(i,j)$. $(\cdot)^*$, $(\cdot)^H$, $|\cdot|$ and $\|\cdot\|_F$ represent the complex conjugate, Hermitian, Euclidean and Frobenius norm operations, respectively. $\Re(j)$, $\Im(j)$, $(\cdot)!$, $\lfloor\cdot\rfloor$, $round(\cdot)$ and $mod(\cdot,\cdot)$ are the real part of complex number j, imaginary part of complex number j, the factorial, the floor operator, round towards the nearest integer and the modulus operator, respectively. I_N is the $N \times N$ identity matrix, $sign(\cdot)$ returns the sign of the argument, and $diag(\boldsymbol{x})$ is a square diagonal matrix with elements of the vector $\boldsymbol{x}$. $Trace(\boldsymbol{X})$ returns the sum of the diagonals of $\boldsymbol{X}$. $argmin_{\omega}(\cdot)$ returns the minimum of an argument with respect to ω, and $argmax_{\omega}(\cdot)$ returns the maximum of an argument with respect to ω.

2. System Model of DSM

2.1. DSM-PSK

Consider a DSM system with N_t transmit antennas, N_r receive antennas, and an M-PSK constellation, χ, of normalized power. There are a total of $N_t!$ AMs, of which only $Q = 2^{\lfloor \log_2(N_t!) \rfloor}$ may be used to transmit information bits. Each antenna matrix $\boldsymbol{AM}_q$ ($q \in [1{:}\,Q]$), is an $N_t \times N_t$ matrix which contains a single non-zero element in each column. For each AM there is an AI vector $\boldsymbol{l}_q = [l_q^1, l_q^2, \dots, l_q^{N_t}]$ where $l_q^n, n \in [1{:}\,N_t]$, is the AI of the active transmit antenna in the n^{th} column of $\boldsymbol{AM}_q$. For example, the set $\boldsymbol{AM}_q$ is given by $\boldsymbol{AM}_1 = \begin{bmatrix} 1 & 0 \\ 0 & 1 \end{bmatrix}$ and $\boldsymbol{AM}_2 = \begin{bmatrix} 0 & 1 \\ 1 & 0 \end{bmatrix}$, for $N_t = 2$ and $Q = 2$, and the AI vector for $\boldsymbol{AM}_2$ is $\boldsymbol{l}_2 = [2, 1]$.

Each transmitted block conveys a total of $B = \log_2(Q) + N_t \log_2(M)$ bits, of which $b_1 = \log_2(Q)$ bits are used to map a single AM, $\boldsymbol{AM}_q$, and $b_2 = N_t \log_2(M)$ bits are used to determine

N_t modulated symbols, s_l ($l \in [1{:}\,N_t]$), which are drawn from χ. The spectral efficiency is therefore $\eta_{DSM-PSK} = (\lfloor \log_2(N_t!) \rfloor + N_t \log_2(M)) \frac{1}{N_t}$ bits/s/Hz.

With this, the t^{th} space-time $N_t \times N_t$ information matrix may be expressed as:

$$\boldsymbol{S}^{(t)} = \boldsymbol{A}\boldsymbol{M}_q diag\left(\boldsymbol{s}^{(t)}\right), \tag{B.1}$$

where the symbol vector , $\boldsymbol{s}^{(t)} = \left[s_1, \dots, s_{N_t}\right]$.

Then the $N_t \times N_t$ differential transmission matrix is defined by:

$$\boldsymbol{X}^{(t)} = \boldsymbol{X}^{(t-1)}\boldsymbol{S}^{(t)}, \tag{B.2}$$

where $\boldsymbol{X}^{(0)} = \boldsymbol{I}_{N_t}$.

The received signal $\boldsymbol{Y}^{(t)} \in \mathbb{C}^{N_r \times N_t}$ over time slots $(t-1)N_t + 1$ to tN_t is given by:

$$\boldsymbol{Y}^{(t)} = \boldsymbol{H}^{(t)}\boldsymbol{X}^{(t)} + \boldsymbol{N}^{(t)}, \tag{B.3}$$

where $\boldsymbol{H}^{(t)} \in \mathbb{C}^{N_r \times N_t}$ and $\boldsymbol{N}^{(t)} \in \mathbb{C}^{N_r \times N_t}$ denote the frequency-flat Rayleigh fading channel, and the noise matrix, respectively. The entries of $\boldsymbol{H}^{(t)}$ and $\boldsymbol{N}^{(t)}$ are independent and identically distributed (i.i.d) random variables with complex Gaussian distributions $\mathcal{CN}(0,1)$ and $\mathcal{CN}(0, \sigma^2)$, respectively.

Assuming quasi-static fading, in which case $\boldsymbol{H}^{(t-1)} = \boldsymbol{H}^{(t)}$, and using (B.2), the received signal $\boldsymbol{Y}^{(t)}$ can be represented as:

$$\boldsymbol{Y}^{(t)} = \boldsymbol{Y}^{(t-1)}\boldsymbol{S}^{(t)} + \widehat{\boldsymbol{N}}^{(t)}, \tag{B.4}$$

where $\boldsymbol{Y}^{(t-1)} = \boldsymbol{H}^{(t-1)}\boldsymbol{X}^{(t-1)} + \boldsymbol{N}^{(t-1)}$ and $\widehat{\boldsymbol{N}}^{(t)} = \boldsymbol{N}^{(t)} - \boldsymbol{N}^{(t-1)}\boldsymbol{S}^{(t)}$.

The optimal ML detector is then given by:

$$\left\{\hat{q}, \hat{\boldsymbol{s}}^{(t)}\right\} = \underset{\substack{\forall \hat{q} \\ \{\hat{s}_l \in \chi\}_{l=1}^{N_t}}}{\operatorname{argmin}} \left\| \boldsymbol{Y}^{(t)} - \boldsymbol{Y}^{(t-1)} \widehat{\boldsymbol{S}}^{(t)} \right\|_F^2, \tag{B.5}$$

and is further derived as [7]:

$$\left\{\hat{q}, \hat{\boldsymbol{s}}^{(t)}\right\} = \underset{\substack{\forall \hat{q} \\ \{\hat{s}_l \in \chi\}_{l=1}^{N_t}}}{\operatorname{argmax}} Trace\left\{\Re\left\{\left(\boldsymbol{Y}^{(t)}\right)^H \boldsymbol{Y}^{(t-1)} \widehat{\boldsymbol{S}}^{(t)}\right\}\right\}. \tag{B.6}$$

The ML detector performs an exhaustive search of all AMs and M-PSK symbols, with the search size spanning a total of QM^{N_t} different combinations.

2.2. DSM-APSK

We now introduce the system model for DSM with APSK modulation, given in [8, Method 1]. The M-M APSK constellation comprises of two M-PSK constellations of different amplitude. The amplitude of the smaller and larger constellation, is set to $r_L = 0.632$ and $r_H = 1.265$, respectively, which satisfy the ratio criterion, $\frac{r_H}{r_L} = 2$ [8].

DSM-APSK transmits a total of $B + 1$ bits in each space-time block, of which B bits determine the AM and the symbols to be transmitted, and the extra bit, defined as $b_3 \in [0, 1]$, selects the amplitude level. Therefore, the spectral efficiency of DSM-APSK is $\eta_{DSM-APSK} = (\lfloor \log_2(N_t!) \rfloor + N_t \log_2(M) + 1) \frac{1}{N_t}$ bits/s/Hz [8].

With this, the differential transmission matrix given by (B.2), for the t^{th} space-time block, is rewritten as [8]:

$$\boldsymbol{X}^{(t)} = \alpha^{(t)} \boldsymbol{X}^{(t-1)} \boldsymbol{S}^{(t)}, \tag{B.7}$$

where

$$\alpha^{(t)} = \begin{cases} 1, & \text{if } b_3 = 0 \\ \frac{r_H}{r_L}, & \text{if } b_3 = 1 \text{ and } \alpha^{(t-1)} = r_L \\ \frac{r_L}{r_H}, & \text{if } b_3 = 1 \text{ and } \alpha^{(t-1)} = r_H \end{cases}, \tag{B.8}$$

and $\alpha^{(0)} = r_L$.

The received signal, $\boldsymbol{Y}^{(t)} \in \mathbb{C}^{N_r \times N_t}$, is then calculated similarly to (B.3), and may be rewritten in terms of the received signal in the $(t-1)^{th}$ block, as:

$$\boldsymbol{Y}^{(t)} = \alpha^{(t)} \boldsymbol{Y}^{(t-1)} \boldsymbol{S}^{(t)} + \widehat{\boldsymbol{N}}^{(t)}, \tag{B.9}$$

where $\boldsymbol{Y}^{(t-1)} = \boldsymbol{H}^{(t-1)} \boldsymbol{X}^{(t-1)} + \boldsymbol{N}^{(t-1)}$ and $\widehat{\boldsymbol{N}}^{(t)} = \boldsymbol{N}^{(t)} - \alpha^{(t)} \boldsymbol{N}^{(t-1)} \boldsymbol{S}^{(t)}$.

Based on (B.9), the ML detector is derived similarly to (B.5) as:

$$\{\hat{q}, \hat{\boldsymbol{s}}^{(t)}, \hat{\alpha}^{(t)}\} = \underset{\substack{\forall \hat{q} \\ \{\hat{s}_l \in \chi\}_{l=1}^{N_t} \\ \forall \hat{\alpha}}}{\operatorname{argmin}} \left\| \boldsymbol{Y}^{(t)} - \hat{\alpha}^{(t)} \boldsymbol{Y}^{(t-1)} \widehat{\boldsymbol{S}}^{(t)} \right\|_F^2. \tag{B.10}$$

Since the initial value of $\alpha^{(0)}$ is known, the ML detector need only search through two possible values of $\hat{\alpha}$ which is dependent on $\hat{\alpha}^{(t-1)}$ [8]. These are either $\hat{\alpha} \in \left[1, \frac{r_L}{r_H}\right]$ or $\hat{\alpha} \in \left[1, \frac{r_H}{r_L}\right]$ [8]. Therefore, the ML detector performs an exhaustive search over $2QM^{N_t}$ combinations.

3. Existing Low-Complexity DSM-PSK Detection Schemes

3.1. Conditionally Optimal Low-Complexity Detection Scheme for DSM [9]

The low-complexity detection scheme proposed in [9] first estimates the N_t AIs which form an AI vector $\hat{\boldsymbol{l}}^{(t)}$, and then the corresponding symbol vector, $\hat{\boldsymbol{s}}^{(t)}$, for each space-time block. In (B.3), the i^{th} column of the received signal, $\boldsymbol{Y}_i^{(t)}$ ($i \in [1{:}\, N_t]$), can be expressed as [9]:

$$\boldsymbol{Y}_i^{(t)} = \boldsymbol{Y}^{(t-1)} \boldsymbol{S}_i^{(t)} + \widehat{\boldsymbol{N}}_i^{(t)}. \tag{B.11}$$

Since $\boldsymbol{S}_i^{(t)}$ contains a single non-zero element, the active antenna index and symbol can be estimated using the HL-ML detection as [9]:

$$\{\hat{l}_i, \hat{s}_i\} = \underset{l_i \in [1,\ldots,N_t]}{\operatorname{argmin}} \left(\left| y_{l_i}^{(t)} - \hat{s}_i \right|^2 - \left| y_{l_i}^{(t)} \right|^2 \right) \left\| \boldsymbol{Y}_{l_i}^{(t-1)} \right\|_F^2, \tag{B.12}$$

where

$$y_{l_i}^{(t)} = \frac{\left(\boldsymbol{Y}_{l_i}^{(t-1)} \right)^H \boldsymbol{Y}_i^{(t)}}{\left(\boldsymbol{Y}_{l_i}^{(t-1)} \right)^H \boldsymbol{Y}_{l_i}^{(t-1)}}, \qquad \hat{s}_i = \mathbb{Q}\left(y_{l_i}^{(t)} \right), \tag{B.13}$$

where $\mathbb{Q}$ denotes the digital demodulation function [9].

Once N_t AIs are estimated, the AI vector $\hat{\boldsymbol{l}}^{(t)}$ can be composed. The number of identical elements between $\hat{\boldsymbol{l}}^{(t)}$ and $\boldsymbol{l}_q$ can then be given as [9]:

$$\boldsymbol{n} = [n_1, \cdots, n_Q]. \tag{B.14}$$

The elements of $\boldsymbol{n}$ are then sorted into descending order as $\hat{\boldsymbol{n}} = [\hat{n}_1, \ldots, \hat{n}_Q]$ and the corresponding index order is [9]:

$$\boldsymbol{m} = [m_1, \cdots, m_Q], \tag{B.15}$$

where m_j ($j \in [1{:}\, Q]$) denotes the index of $\hat{n}_j$, respectively.

If $\hat{n}_1 = N_t$, then the obtained $\hat{\boldsymbol{l}}^{(t)}$ is a legitimate solution, therefore, the final result is $(m_1, \hat{\boldsymbol{s}}^{(t)})$. If $\hat{n}_1 < N_t$, then $\hat{\boldsymbol{l}}^{(t)}$ is considered an illegitimate solution. P_M is then given as the number of the largest elements in $\boldsymbol{n}$ [9]. The first P ($P \geq P_M$) AMs in (B.15) are then chosen for detection using the ML detector, and is given by [9]:

$$\hat{q} = \underset{\tilde{q} \in [m_1,\ldots,m_P]}{\operatorname{argmin}} \left\| \boldsymbol{Y}^{(t)} - \boldsymbol{Y}^{(t-1)} \boldsymbol{A} \boldsymbol{M}_{\tilde{q}} diag\left(\hat{\boldsymbol{s}}_{\tilde{q}}\right) \right\|_F^2, \tag{B.16}$$

where the corresponding $\hat{\boldsymbol{s}}_q$ is obtained using (B.13).

3.2. A Suboptimal Low-Complexity DSM Detector [10]

In [10], a low-complexity near-ML DSM detector is proposed. The first step involves the initial detection of the modulated symbols. Let $\boldsymbol{W}^{(t)} = \boldsymbol{Y}^{(t)^H} \boldsymbol{Y}^{(t-1)}$, $\boldsymbol{W}^{(t)} \in \mathbb{C}^{N_t \times N_t}$. For brevity, we will now omit the t notation. The modulated symbols transmitted in the different time slots are independent of one another and as a result (B.6) can be written as [10]:

$$\begin{aligned} \hat{G}(i,j) &= \underset{\hat{s} \in \chi}{\operatorname{argmax}} \left\{ \Re\{W(i,j)\hat{s}\} \right\} \\ &= \underset{\hat{s} \in \chi}{\operatorname{argmax}} \left\{ \Re\{W(i,j)\}\Re\{\hat{s}\} - \Im\{W(i,j)\}\Im\{\hat{s}\} \right\}. \end{aligned} \tag{B.17}$$

The detection scheme exploits the symmetric nature of the PSK constellation, and searches for symbol $\hat{s}$ in the first quadrant, which satisfies [10]:

$$\hat{D}(i,j) = |\Re\{W(i,j)\}|\Re\{\hat{s}\} + |\Im\{W(i,j)\}|\Im\{\hat{s}\}. \tag{B.18}$$

The complexity can be reduced since the real and imaginary parts of the symbols are symmetric. In [10], this is shown by first defining $\Delta(i,j) = 0$ if $|\Re\{W(i,j)\}| > |\Im\{W(i,j)\}|$, otherwise $\Delta(i,j) = 1$. Let $\hat{s} = e^{j\frac{2\pi}{M}(K'(i,j) + \frac{M}{8}\Delta(i,j))}$ and $\hat{G}(i,j) = e^{j\frac{2\pi}{M}K(i,j)}$ [10]. It is clear that $\hat{s}$ and $\hat{G}(i,j)$ may be determined by calculating $K'(i,j)$ and $K(i,j)$, respectively, which are given by [10]:

$$K'(i,j) = \underset{k \in \left[0,\ldots,\frac{M}{8}\right]}{\operatorname{argmax}} \{|\Re\{W(i,j)\}| \cos(a) + |\Im\{W(i,j)\}| \sin(a)\}, \tag{B.19}$$

$$K(i,j) = \frac{M}{4}\left(2 + sign\left\{\Im\{W(i,j)\}\right\} + b\right) - b\left(K'(i,j) + \frac{M}{8}\Delta(i,j)\right), \tag{B.20}$$

where $a = \frac{2\pi}{M}k + \frac{\pi}{4}\Delta(i,j)$ and $b = \frac{sign\{\Re\{W(i,j)\}\}}{sign\{\Im\{W(i,j)\}\}}$.

Once $\widehat{\boldsymbol{G}}$ is computed using (B.20), the metric matrix $\widehat{\boldsymbol{D}}$ can be obtained via (B.18).

The second step involves estimation of the AM index $\hat{q}$ via [10]:

$$\hat{q} = \underset{\tilde{q}\in[1,\ldots,(N_t-1)(N_t-1)!]}{\operatorname{argmax}} \left\{\sum_{i=1}^{N_t} \widehat{D}\left(i, \boldsymbol{l}_{\tilde{q}}(i)\right)\right\}. \tag{B.21}$$

Given $\hat{q}$, the signal domain detection is then simply given by $\hat{s}_n = \hat{G}\left(n, \boldsymbol{l}_{\tilde{q}}(n)\right), n \in [1{:}\, N_t]$. For large N_t, $(N_t \geq 3)$, the AM index estimation is carried out in a manner similar to the Viterbi decoder [10]. The algorithm is omitted as it does not contribute to the computational complexity of the detector.

4. Proposed Low-Complexity Near-ML Detector

In this section, we propose a simple low-complexity near-ML detector for DSM with an M-PSK or M-M APSK constellation. The proposed detector is highly dependent on the structure of the M-PSK constellation, therefore, we first discuss the important properties of the constellation and its relation to the M-M APSK constellation.

4.1. PSK Constellation

In Figure B.1.a, as is well-known, the M-PSK symbols have a fixed amplitude, generally equal to 1. Due to the constant amplitude, information is encoded in the phase of the symbols [13]. The n^{th} M-PSK symbol can be expressed as [12-13]:

$$s_n = Ae^{j\phi_n}\,,\ n \in [1{:}\, M], \tag{B.22}$$

where $A = 1$ is the amplitude of the constellation points, and $\phi_n = (n-1)\frac{2\pi}{M}$ is the phase of the n^{th} M-PSK symbol, respectively. We can then define the look-up table $LUT = [s_1, \ldots, s_M]$.

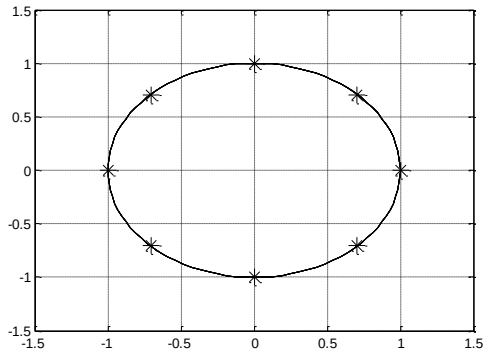

Figure B.1.a: 8-PSK constellation [12]

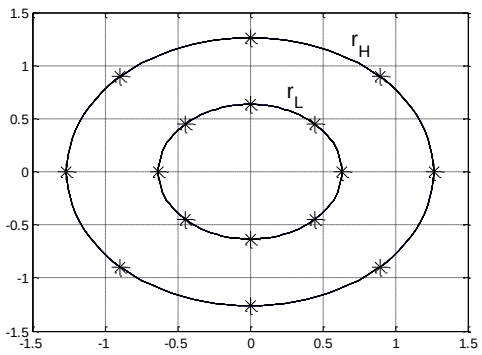

Figure B.1.b: 8-8 APSK constellation [8]

Detection of the n^{th} M-PSK symbol s_n is equivalent to detection of ϕ_n. Each symbol in the constellation has a detection region φ_n. The detection region φ_n for the n^{th} M-PSK symbol is bounded as $\left[\phi_n - \frac{\pi}{M}, \phi_n + \frac{\pi}{M}\right]$ [13]. If the phase of a received signal lies within the detection region φ_n, then the receiver estimates the transmitted symbol as the n^{th} M-PSK symbol.

The M-M APSK constellation in Figure B.1.b, may be thought of as two identical M-PSK constellations, initially with $A = 1$, which are then scaled by a factor of $A = r_L$ and $A = r_H$, respectively. Therefore, it is obvious that although the n^{th} symbol in the two constellations have different amplitudes, their phase is the same. As a result, the detection region concept may be applied to the M-M APSK constellation, to reduce the signal domain search space to the two symbols, whose phase is closest to that of the received signal.

4.2. A Simple Low-Complexity Near-ML Detection Algorithm for DSM-PSK

For convenience we denote $W(i,j)$ and $\hat{s}(i,j)$ in (B.17) as $W(i,j) = re^{j\theta}$ and $\hat{s}(i,j) = e^{j\phi}$ in polar form, then (B.17) becomes:

$$\begin{aligned} \hat{G}(i,j) &= \underset{\phi \in \Psi}{\operatorname{argmax}} \left\{ \Re\left\{ re^{j(\theta+\phi)} \right\} \right\} \\ &= \underset{\phi \in \Psi}{\operatorname{argmax}} \{\cos(\theta + \phi)\}, \end{aligned} \tag{B.23}$$

where $\Psi = \{\phi_n\}_{n=1}^{M}$.

In order to maximize (B.23), we have $\theta + \phi = 0$, and therefore $\phi = -\theta$, i.e. the smaller the angle between $(W(i,j))^*$ and $\hat{s}(i,j)$, the larger $\cos(\theta + \phi)$ is [12]. This property is exploited in the proposed detection scheme to significantly reduce the complexity of the detector, since only a specific symbol is required to maximize (B.17), thus eliminating the need for an exhaustive search of the constellation set.

Let $L_{\hat{\phi}} = \frac{-\theta}{2\pi/M}$ [12], then the index of the detected M-PSK symbol can be estimated using a modified version of [12, (10)]:

$$\hat{n} = 1 + mod\left(round\left(L_{\hat{\phi}}\right), M\right). \tag{B.24}$$

Using the result from (B.24), the corresponding symbol $\hat{s}(i,j)$, may be simply obtained from LUT, and is used to compose the estimated symbol matrix $\widehat{\boldsymbol{SM}} \in \mathbb{C}^{N_t \times N_t}$.

Once the transmitted symbols are estimated, it is straightforward to obtain the matrix $\widehat{\boldsymbol{G}}$ from (B.17). Then the AM index used during transmission is estimated, similarly to (B.21), using the following expression:

$$\hat{q} = \underset{q \in Q}{\operatorname{argmax}} \left\{ \sum_{i=1}^{N_t} \widehat{\boldsymbol{G}}(i, \boldsymbol{l}_q(i)) \right\}. \tag{B.25}$$

Finally, the estimated symbol transmitted from each antenna is simply $\hat{s}_i = \widehat{SM}\{i, \boldsymbol{l}_{\hat{q}}(i)\}$, where $i \in [1{:}\, N_t]$.

4.3. A Simple Low-Complexity Near-ML Detection Algorithm for DSM-APSK

The proposed low-complexity near-ML detector for DSM-APSK, uses a similar algorithm to that proposed for DSM-PSK.

Initially, we assume that the APSK constellation consists of a single M-PSK constellation with $A = 1$. This simplifies the estimation of the transmitted symbol indices and the AM index, via the use of (B.24) and (B.25), respectively. Thereafter, using the estimated symbols for the M-PSK constellation, $\hat{s}_i$ ($i \in [1{:}\, N_t]$), we compose the estimated symbol vector $\hat{\boldsymbol{s}}^{(t)}$. It is then possible to obtain the estimated information matrix, $\widehat{\boldsymbol{S}}^{(t)}$, using (B.1). With this, a modified ML detector is derived from (B.10), to estimate $\hat{\alpha}^{(t)}$. The modified ML detector is given by:

$$\{\hat{\alpha}^{(t)}\} = \underset{\forall \hat{\alpha}}{\operatorname{argmin}} \left\| \boldsymbol{Y}^{(t)} - \hat{\alpha}^{(t)} \boldsymbol{Y}^{(t-1)} \widehat{\boldsymbol{S}}^{(t)} \right\|_F^2. \quad \text{(B.26)}$$

Since $\alpha^{(0)}$ is known, the ML detector need only search through two possible values of $\hat{\alpha}$, as mentioned in Section 2.2.

5. Complexity Analysis

In this section, we analyze the complexity of the proposed detection scheme for PSK and APSK modulation. We then compare the complexity of the proposed low-complexity DSM-PSK detector, to that of the conventional ML detector and the existing low-complexity detection schemes for PSK. Additionally, the complexity of the proposed detector for APSK is compared to its respective ML detector.

The complexity of the proposed detectors are derived using the concept of computational complexity as in [9], which is defined as the total number of real-valued multiplications in a given algorithm. Note that multiplication of two complex numbers requires a total of 4 real-valued multiplications.

5.1. Proposed Low-Complexity Detector for DSM-PSK

For a single space-time block, the computational complexity of the proposed low-complexity detector for DSM-PSK, is derived as follows.

1. To compute $\boldsymbol{W}^{(t)} = \boldsymbol{Y}^{(t)^H} \boldsymbol{Y}^{(t-1)}$, we first reduce the entries in $\boldsymbol{Y}^{(t)^H}$ and $\boldsymbol{Y}^{(t-1)}$ to polar form. This requires $2N_r N_t$ real-valued multiplications to determine the magnitude of each complex entry, in each of the matrices. The phase may be obtained via a look-up table without adding to the overall complexity. Computing the matrix multiplication, $\boldsymbol{Y}^{(t)^H} \boldsymbol{Y}^{(t-1)}$, then requires a further $3N_r N_t^2$ real-valued multiplications. Thereafter, only the phase of each entry in $\boldsymbol{W}^{(t)}$ is required. The total computational complexity incurred in computing $\boldsymbol{W}^{(t)}$ is, $4N_r N_t + 3N_r N_t^2$ real-valued multiplications.
2. Each computation of $L_{\widehat{\phi}}$ requires 1 real-valued multiplication, since $\frac{-1}{2\pi/M}$ is regarded as a constant. Therefore, computing $L_{\widehat{\phi}}$ for the entirety of $\boldsymbol{W}^{(t)}$ results in a total computational complexity of ${N_t}^2$ real-valued multiplications.

3. For each calculation of $\hat{n}$ in (B.24), the $mod(\cdot,\cdot)$ operation requires 2 real-valued multiplications. Therefore, calculating calculate $\hat{n}$ for the entirety of $\boldsymbol{W}^{(t)}$ requires $2{N_t}^2$ real-valued multiplications.
4. Finally from (B.17), the calculation of $\widehat{\boldsymbol{G}}$ requires $2{N_t}^2$ real-valued multiplications.

Therefore, the overall computational complexity of the proposed low-complexity DSM-PSK detector, is $C_{Proposed-PSK} = 4N_rN_t + 3N_rN_t^2 + 5{N_t}^2$ real-valued multiplications.

5.2. Proposed Low-Complexity Detector for DSM-APSK

Since the proposed detector for DSM-APSK utilizes the same algorithm as the proposed DSM-PSK detector, the computational complexity incurred when estimating the symbols and AM index, is $4N_rN_t + 3N_rN_t^2 + 5{N_t}^2$ real-valued multiplications. The additional complexity incurred when estimating $\hat{\alpha}^{(t)}$ via the modified ML detector in (B.26), is detailed as follows.

1. Computing $\widehat{\boldsymbol{S}}^{(t)}$ via (B.1), requires 4 real-valued multiplications.
2. Thereafter, computing the matrix multiplication, $\boldsymbol{Y}^{(t-1)}\widehat{\boldsymbol{S}}^{(t)}$, incurs a total of $4N_rN_t$ real-valued multiplications.
3. The resulting matrix is then multiplied by $\hat{\alpha}$, which incurs a further $2N_rN_t$, real-valued multiplications.
4. Finally, the Frobenius norm requires 2 real-valued to compute a single entry in the matrix. Therefore, for the entirety of the resultant matrix, a total of $2N_rN_t$ real-valued multiplications are required.

The ML detector searches through two possible values of $\hat{\alpha}$ in each space-time block. However, the result of $\boldsymbol{Y}^{(t-1)}\widehat{\boldsymbol{S}}^{(t)}$ does not change during a block, therefore, it is only required to be calculated once. With this, the total computational complexity of the ML detector is $12N_rN_t + 4$ real-valued multiplications.

Therefore, the total computational complexity of the proposed detector for DSM-APSK is $C_{Proposed-APSK} = 16N_rN_t + 3N_rN_t^2 + 5{N_t}^2 + 4$.

5.3. Discussion on Computational Complexity of the Presented Detectors

In Table B.1, we provide the computational complexity of the existing detection schemes for DSM. The proposed detection scheme, unlike the detection schemes in [9] and [10], is independent of M and Q, for PSK and APSK modulation. Note that for the low-complexity

detection scheme in [9], γ_1 and γ_2, $(\gamma_1 + \gamma_2 = 1)$, denote the percentages of legitimate and illegitimate $\hat{\boldsymbol{l}}^{(t)}$, respectively.

Assuming a high SNR, in which case $\gamma_1 = 100\%$, we observe in Table B.2 that the proposed low-complexity detection scheme for DSM-PSK achieves at least 98% reduction in computational complexity over the ML detector, and a considerable reduction over the detection schemes in [9] and [10]; for example, a 35% reduction is realized over both detectors for $N_r = 2$, $N_t = 4$ and 8-PSK modulation. It can be deduced from Table B.1, that at lower SNRs, where $\gamma_1 \neq 100\%$, and with $P = Q$, the proposed detection scheme would yield a greater percentage reduction in computational complexity over [9], than that given in Table B.2, while achieving optimal ML error performance.

Table B.1: Comparison of the Existing Detection Schemes Conceived for DSM

Detection Scheme	**ML Optimality**	**Computational Complexity**
DSM-PSK ML Detector	Optimal	$C_{ML} = (4N_rN_t + 2N_rN_t)QM^{N_t}$
DSM-APSK ML Detector	Optimal	$C_{ML} = (4N_rN_t + 2N_rN_t)2QM^{N_t}$
PSK Detector in [9]	Conditionally Optimal $(P = Q)$	$C_{[9]} = \gamma_1\left(2N_rN_t + 4N_rN_t{}^2 + 11N_t{}^2\right) + \gamma_2\begin{pmatrix}2N_rN_t + 4N_rN_t{}^2 + 11N_t{}^2 + \\ \left(2N_rN_t + 4N_rN_t{}^2\right)P\end{pmatrix}$
PSK Detector in [10]	Sub-optimal	$C_{[10]} = 4N_rN_t^2 + 2\left(\frac{M}{8} + 1\right)N_t{}^2 + 8N_t{}^2$
Proposed DSM-PSK Detector	Optimal	$C_{Proposed-PSK} = 3N_rN_t^2 + 4N_rN_t + 5N_t{}^2$
Proposed DSM-APSK Detector	Optimal	$C_{Proposed-APSK} = 3N_rN_t^2 + 16N_rN_t + 5N_t{}^2 + 4$

Furthermore, in Table B.3, the proposed low-complexity detector for DSM-APSK is shown to achieve a significant reduction in complexity, compared to the ML detector. At least a 98% reduction in computational complexity is realized.

Table B.2: Percentage Reduction in Computational Complexity of Proposed DSM-PSK Detector Relative to Existing Detection Schemes

System Configuration			**Percentage Reduction** (%)		
N_r	N_t	M	ML	[9]	[10]
2	2	16	99	29	32
2	2	8	98	29	25
2	4	8	99.9	35	35
2	8	8	99.9	38	40
4	8	8	99.9	32	32

Table B.3: Comparison between Proposed Low-complexity Detector and the ML Detector for DSM-APSK

System Configuration			**Computational Complexity**		% **Reduction**
N_r	N_t	M	ML	Proposed	
2	2	16	24,576	112	99.5
2	2	8	6,144	112	98.2
2	4	8	6.29×10^6	308	99.9
2	8	8	1.05×10^{14}	964	99.9
4	8	8	2.11×10^{14}	1,604	99.9

6. Simulation Results

In this section, Monte-Carlo simulations are carried out to determine the error performance of the proposed DSM-PSK and DSM-APSK detection schemes. These are compared with the current low-complexity DSM-PSK detectors in [9] and [10], and the ML detector for DSM-APSK, respectively. Different system configurations are simulated to obtain a clear understanding of the error performance, of the various detectors.

It is clear from Figure B.2 and Figure B.3 that the proposed low-complexity detector, for DSM-PSK, yields near-ML performance throughout the SNR range for the various configurations. The proposed detector yields marginally better performance at low SNRs as compared to the detector in [10], which may be due to the detector in [10] using more than Q AMs to estimate the AM

index and as a result the estimated index may not be included in Q. It is also noted that the proposed detector yields better performance than the detector in [9] at lower SNRs for larger N_t, since at low SNRs, there are inaccurate AIs in $\hat{\boldsymbol{l}}^{(t)}$ [9]. As a result, the detector in [9] experiences an error performance loss and an increase in computational complexity, since the accurate AM may not lie within the selected P_M AMs and $\gamma_1 \neq 100\%$, respectively.

In Figure B.4 and Figure B.5, it is demonstrated that the proposed low-complexity detector, for DSM-APSK, achieves near-ML error performance, down to a bit error rate (BER) of 10^{-5}, for the various system configurations.

From the results, we can conclude, that the proposed detectors offer a significant reduction in computational complexity as compared to the ML detector, and existing low-complexity detectors, while achieving near-ML error performance throughout the SNR range.

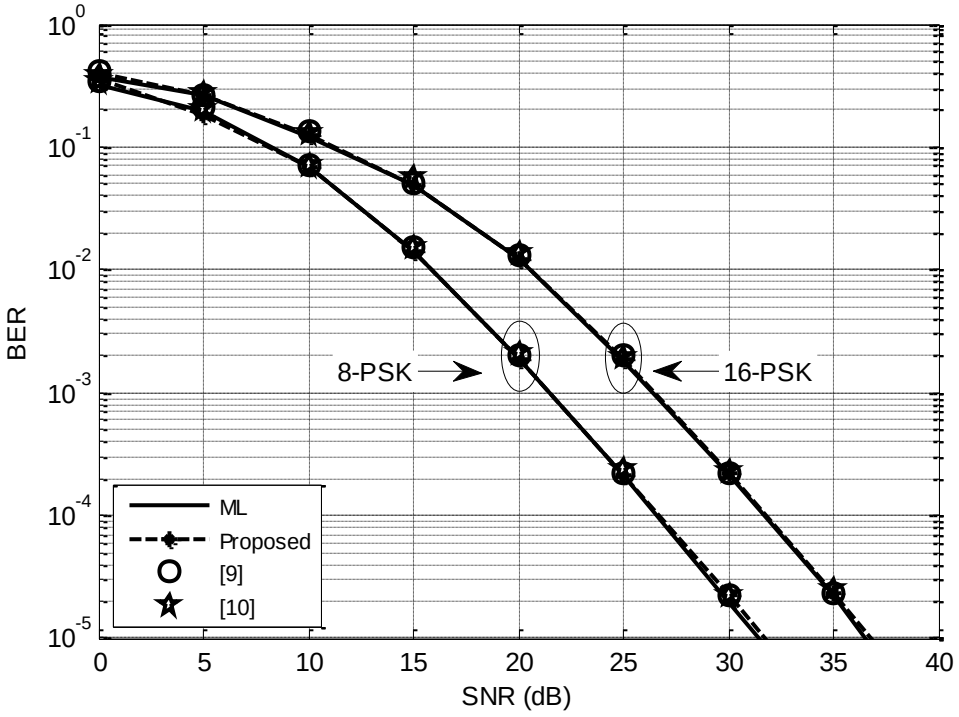

Figure B.2: DSM M-PSK BER performance with $N_r = 2$, $N_t = 2$.

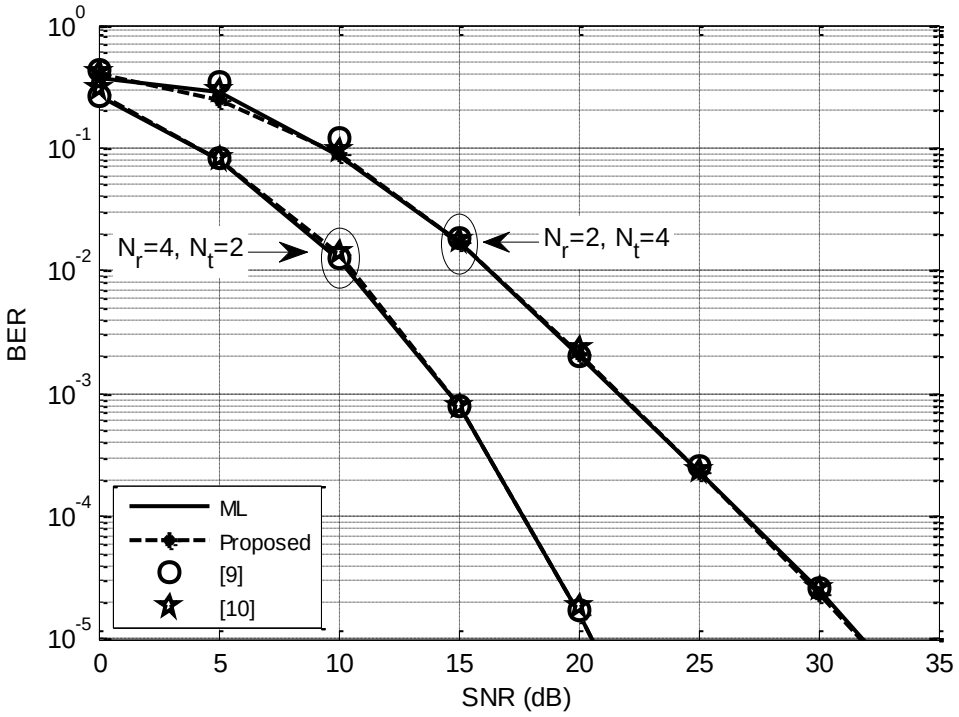

Figure B.3: DSM 8-PSK BER performance for various antenna configurations.

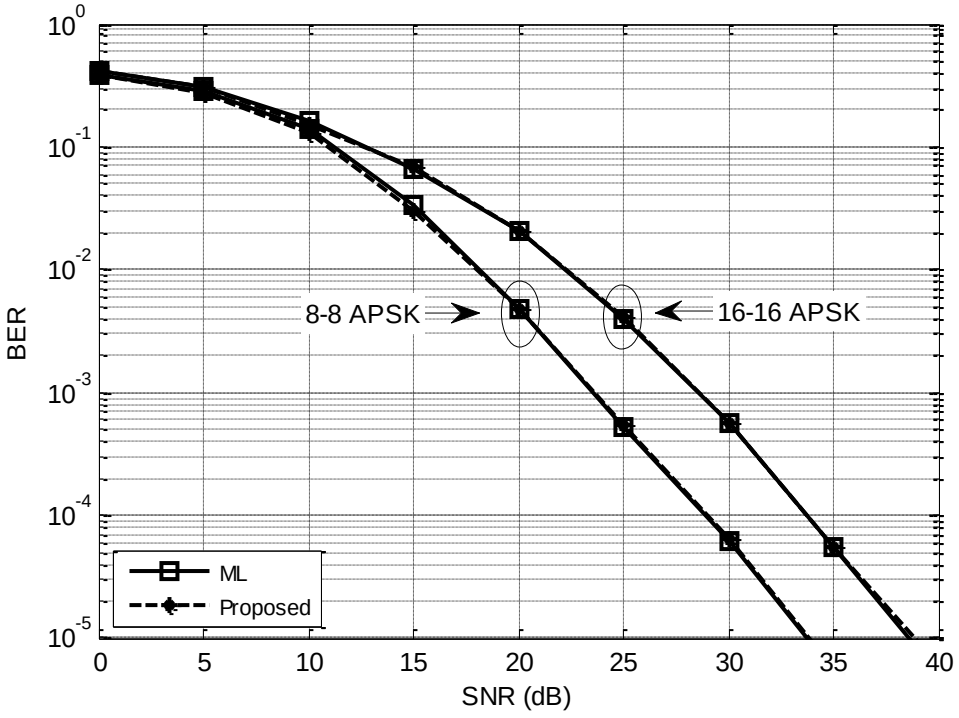

Figure B.4: DSM M-M APSK BER performance with $N_r = 2, N_t = 2$.

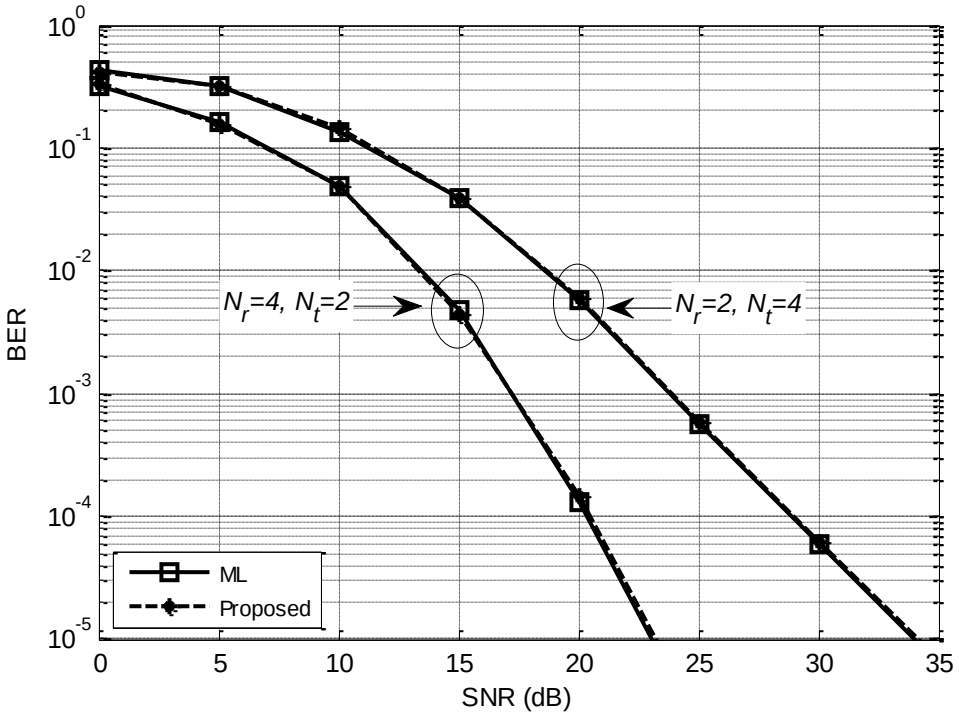

Figure B.5: DSM 8-8 APSK BER performance for various antenna configurations.

7. Conclusion

A simple, low-complexity detection scheme is proposed for DSM with *M*-PSK modulation, which manipulates the phase of the received signals in order to demodulate and estimate the transmitted symbols and the index of the antenna matrix. Additionally, we modify and apply the proposed detection algorithm to DSM with *M-M* APSK modulation. Simulation results demonstrate that the detectors are capable of achieving near-ML performance with significantly lower computational complexity than that of the respective ML detection schemes, and current low-complexity detectors.

References

[1] R. Y. Mesleh, H. Haas, S. Sinanovic, C.W. Ahn, and S.Yun, "Spatial Modulation," *IEEE Trans. Veh. Tech.*, vol. 57, no. 4, pp. 2228 – 2242, Jul. 2008.

[2] R. Y. Mesleh, H. Haas, C. W. Ahn, and S. Yun, "Spatial Modulation – A New Low Complexity Spectral Efficiency Enhancing Technique," *in Proc. of the Conf. on Commun. and Netw., China*, pp. 1 – 5, Oct. 2006.

[3] N. Pillay, and H. Xu, "Low Complexity Detection and Transmit Antenna Selection for Spatial Modulation," *SAIEE Africa Research Journal*, vol. 105, no. 1, pp. 4 – 12, Mar. 2014.

[4] S. Sugiura, S. Chen, and L. Hanzo, "Coherent and Differential Space-Time Shift Keying: A Dispersion Matrix Approach," *IEEE Trans. Commun.*, vol. 58, no. 11, pp. 3219 – 3230, Nov. 2010.

[5] Y. Bian, M. Wen, X. Cheng, H. V. Poor, and B. Jiao, "A Differential Scheme for Spatial Modulation," *in Proc. of the IEEE GLOBECOM conf., USA*, pp. 3925 – 3930, Dec. 2013.

[6] N. Ishikawa, and S. Sugiura, "Unified Differential Spatial Modulation," *IEEE Wireless Commun. Lett.*, vol. 3, no. 4, pp. 337 – 340, Aug. 2014.

[7] Y. Biang, X. Cheng, M. Wen, L. Yang, H. V. Poor, and B. Jiao, "Differential Spatial Modulation," *IEEE Trans. Veh. Technol.*, vol. 64, no. 7, pp. 3262 – 3268, Aug. 2014.

[8] P.A. Martin, "Differential Spatial Modulation for APSK in Time-Varying Fading Channels," *IEEE Commun. Lett.*, vol. 19, no. 7, pp. 1261 – 1264, Apr. 2015.

[9] L. Xiao, P. Yang, X. Lei, Y. Xiao, S. Fan, S. Li, and W. Xiang, "A Low-complexity Detection Scheme for Differential Spatial Modulation," *IEEE Commun. Lett.*, vol. 19, no. 9, pp. 1516 – 1519, Jun. 2015.

[10] M. Wen, X. Cheng, Y. Bian, and H. V. Poor, "A Low-Complexity Near-ML Differential Spatial Modulation Detector," *IEEE Signal Process. Lett.*, vol. 22, no. 11, pp. 1834 – 1838, Jun. 2015.

[11] R. Rajashekar, K.V.S. Hari, and L. Hanzo, "Reduced-complexity ML detection and capacity-optimized training for spatial modulation systems," *IEEE Trans. Commun.*, vol. 62, no. 1, pp. 112 – 125, Jan. 2014.

[12] H. Men, and M. Jin, "A Low Complexity ML Detection Algorithm for Spatial Modulation Systems with MPSK Constellation," *IEEE Commun. Lett.*, vol. 18, no. 8, pp. 1375 – 1378, Jun. 2014.

[13] A. Goldsmith, *Wireless Communications*, Cambridge University Press, pp. 135 – 136, 2005.

Part III

Conclusion

Conclusion

This dissertation consists of two papers, which focus on improving the error performance of DSM, as well as providing an alternative, low-complexity detection algorithm, to the computationally intensive DSM ML detector.

In Paper A, the GD-SM and G-DSM schemes were presented, which are based on SM and DSM systems, respectively, with an arbitrary number of transmit and receive antennas. Both schemes employed optimal power allocation and a split frame structure, wherein the first block of a frame (reference block) was transmitted at a higher power than the remaining blocks (normal blocks) of the frame. As a result, the received reference signal provided an enhanced estimation of the channel, which in turn, improved the estimation of the differentially encoded information in the normal blocks. Moreover, the architecture of the frame permitted the use of QAM modulation in the proposed differential schemes, without the need for complex algorithms. The use of QAM modulation is not possible in conventional DSM.

A complexity analysis revealed that the ML detector for G-DSM may achieve up to a 67% reduction in computational complexity compared to the ML detector for conventional DSM. Additionally, a theoretical upper bound on the ABEP was derived for the proposed schemes, and has been shown to closely match the simulation results at high SNRs. A summary of the SNR performance gains for GD-SM and G-DSM over their respective conventional schemes (in which optimal power allocation is not applied), has been presented in Table 1 and Table 2, respectively.

Paper B proposed a simple low-complexity detector for DSM, with PSK and APSK modulation. The detector exploited the property of the PSK constellation, wherein the amplitude of the constellation remains constant, thus, information is encoded only in the phase of the constellation points. The proposed detector manipulated the phase of the received signals to determine the transmitted symbol in each time slot. This was achieved without performing an exhaustive search through all the constellation points. Thereafter, the transmitted AM was determined based on the estimated symbols.

The proposed algorithm was also extended to DSM with APSK modulation. The transmitted symbols and AM were estimated as in the proposed detector for DSM-PSK, however, estimation of the amplitude level required the use of the ML detector, whose search space was reduced to only two possible values.

A complexity analysis validated that the proposed detectors are independent of the constellation size and the number of usable AMs. Furthermore, it was demonstrated that the proposed detector for DSM-PSK achieved at least a 98% reduction in computational complexity over the ML detector, and a considerable reduction over the existing low-complexity detectors. A minimum

reduction of 98% was also realized for DSM-APSK, over the ML detector. Simulation results revealed that both proposed detectors achieved near-ML performance down to a BER of 10^{-5}, throughout the SNR range. This was validated for various antenna configurations and constellation sizes. Therefore, it was concluded, that the detectors achieve significant reductions in computational complexity, while maintaining optimal error performance.

Thus, Papers A and B have presented easily implementable DSM systems, which have satisfied the research objectives.

Table 1: SNR Gain of GD-SM over Conventional GD-SM, at a BER of 10^{-4}

System Configuration			**Conventional**	**GD-SM SNR**	**SNR**
N_t	N_r	**Constellation**	**GD-SM SNR**	$K = 400$	**Gain**
2	2	16-PSK	~31.7 dB	~29.4 dB	~2.3 dB
4	2	16-PSK	~31.5 dB	~29.2 dB	~2.3 dB
2	2	64-QAM	~34.6 dB	~32 dB	~2.6 dB

Table 2: SNR Gain of G-DSM over Conventional DSM, at a BER of 10^{-4}

System Configuration			**Conventional**	**G-DSM SNR**	**SNR**
N_t	N_r	**Constellation**	**DSM SNR**	$K = 400$	**Gain**
4	2	16-PSK	~31.4 dB	~29.0 dB	~2.4 dB
2	2	16-PSK	~31.7 dB	~29.2 dB	~2.5 dB
2	2	16-QAM	~31.7 dB (16-PSK)	~26.2 dB	~5.5 dB